Published by Institute of Physics Publishing for SISSA
Received: *June 7, 2005*
Accepted: *August 1, 2005*
Published: *August 23, 2005*

Duality violations and spectral sum rules

Oscar Catà,[a] **Maarten Golterman**[b] **and Santiago Peris**[a]

[a] *Grup de Física Teòrica and IFAE, Universitat Autònoma de Barcelona 08193 Barcelona, Spain*
[b] *Department of Physics and Astronomy, San Francisco State University 1600 Holloway Ave, San Francisco, CA 94132, U.S.A.*
E-mail: ocata@ifae.es, maarten@aapje.wustl.edu, peris@ifae.es

Abstract: We study the issue of duality violations in the $VV - AA$ vacuum polarization function in the chiral limit. This is done with the help of a model with an expansion in inverse powers of the number of colors, N_c, allowing us to consider resonances with a finite width. Due to these duality violations, the Operator Product Expansion (OPE) and the moments of the spectral function (e.g. the Weinberg sum rules) do not match at finite momentum, and we analyze this difference in detail. We also perform a comparative study of many of the different methods proposed in the literature for the extraction of the OPE parameters and find that, when applied to our model, they all fare quite similarly. In fact, the model strongly suggests that a significant improvement in precision can only be expected after duality violations are included. To this end, we propose a method to parameterize these duality violations. The method works quite well for the model, and we hope that it may also be useful in future determinations of OPE parameters in QCD.

Keywords: 1/N Expansion, Asymptotic Freedom, QCD, Sum Rules.

Contents

1. Introduction

The Operator Product Expansion (OPE) [1] is of paramount importance in QCD because it is the short-distance window not only to fundamental parameters of the lagrangian such as quark masses and the coupling constant α_s, but also to other important quantities not explicitly appearing in the lagrangian, such as the condensates. Moreover, there are cases, like that of the $\Pi_{VV} - \Pi_{AA}$ vacuum polarization, where these condensates turn out to be related to electroweak coupling constants governing the physics of kaon decay and its associated CP violation [2]. It is therefore essential to understand how the OPE works and what its properties of convergence are. It is clear that using the expansion in a region without good convergence (or with no convergence at all) may result in errors in the determination of these important parameters.

The OPE in QCD is believed to be only an asymptotic expansion in inverse powers of q^2 in the complex q^2 plane excluding the Minkowski region, $\mathrm{Re}\, q^2 > 0$. However, it is precisely in the Minkowski region where experimental data are available, so that in order for the OPE to make contact with the experimental data, one has to learn how to make the necessary rotation in the complex plane. A famous trick [3], relying on Cauchy's theorem, relates the integral of the spectral function (i.e. of the experimental data) $\rho(t) = (1/\pi)\,\mathrm{Im}\,\Pi(t)$ to that of the corresponding Green's function $\Pi(q^2)$ of complex argument q^2, over the contour of figure 1, chosen counter-clockwise. One finds [4]

$$\int_0^{s_0} dt\ P\left(t\right) \frac{1}{\pi}\,\mathrm{Im}\,\Pi(t) = -\frac{1}{2\pi i} \oint_{|q^2|=s_0} dq^2\ P\left(q^2\right) \Pi(q^2)\,, \tag{1.1}$$

where $P(x)$ is any polynomial. As it stands, eq. (1.1) is of course an exact mathematical statement. The right-hand side of eq. (1.1), however, contains the full Green's function $\Pi(q^2)$ which is not available in QCD. It is then assumed that, if the contour radius s_0 is large enough, use of the expansion $\Pi_{OPE}(q^2)$ instead of the exact function will be a good enough approximation. This is the rationale underlying all modern analyses in QCD based on the OPE such as e.g. the interesting work of ref. [5].

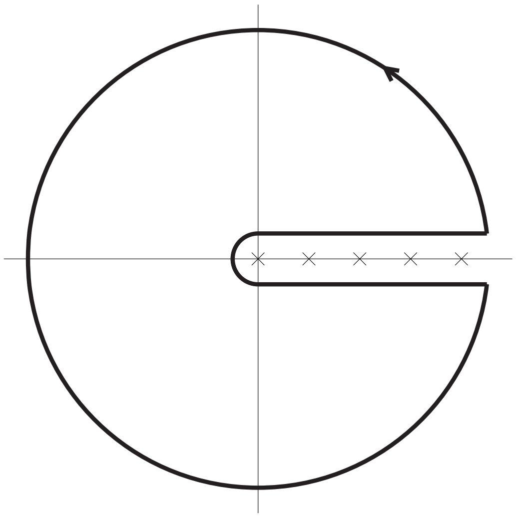

Figure 1: This figure shows the contour in the complex plane leading to eq. (1.1). The crosses on the real axis denote the position of the resonance poles in the $N_c \to \infty$ limit, or the cut arising at finite N_c.

The approximation which consists of substituting $\Pi(q^2) \to \Pi_{OPE}(q^2)$, with s_0 large enough, has been given the name *duality*. Duality refers to the fact that, if the approximation were exact and the substitution $\Pi(q^2) \to \Pi_{OPE}(q^2)$ carried no error, one could say that the integral of the experimental spectral function $\mathrm{Im}\,\Pi(t)$ in eq. (1.1) is dual to the OPE. The term *duality violation*, consequently, refers to any contribution missed by this substitution.

The question is whether this approximation works for large s_0, and if so, how large s_0 should be for duality to apply within a precision of, let us say, 10%? In order to address this question, it is essential to be able to assess the validity of the approximation used, lest the extraction of OPE parameters not be afflicted by uncontrolled systematic errors. Therefore, studying the contribution missed by the replacement $\Pi(q^2) \to \Pi_{OPE}(q^2)$ in eq. (1.1) is a necessary task in the present era of precision determination of QCD parameters.

That the OPE can at best only be an asymptotic expansion in the euclidean region can be most neatly seen in the case of a two-point Green's function made of a pair of quark bilinears, such as the vacuum polarization, in the large-N_c limit [6]. This is because in this limit all meson resonances appear as intermediate physical states with a vanishing width and, consequently, as poles on the positive real axis in the q^2 complex plane. In contrast, the OPE is a series expansion in inverse powers of q^2 (up to logarithms) with no sign of a pole anywhere but at the origin, which means that it cannot converge on the positive real axis. The OPE can thus at best be asymptotic,[1] and even then only provided the positive real axis, i.e. the Minkowski region, is excluded. The region of validity of the expansion, therefore, is expected to be some sort of angular sector around the origin not including the positive real axis. Much less clear are more detailed properties such as, for instance, what the shape of this angular sector may be.

[1] A convergent expansion always has a circular region of convergence characterized by a non-zero radius.

JHEP08(2005)076

Presently, the theory of duality violations in QCD is almost non-existing and it is important to develop it. In the absence of such a theory, we see no other choice but to resort to models. Somewhat surprisingly, not much work has been devoted to this issue. To our knowledge, ref. [7] was the first to point out the importance of duality violations. That the OPE may also miss other important contributions has recently been suggested in ref. [8].

In this work we will study a *model* of duality violations. We hasten to emphasize that our model is *not* QCD. In spite of this, we believe that it shares enough properties with QCD to be an interesting theoretical laboratory for studying issues related to duality violations. After all, our goal here is not a detailed numerical study of duality violations in QCD, but the much more modest one of understanding what the main features are, and how these violations may manifest themselves. This is not just an exercise of purely academic interest, however, because the lessons learned from the model raise questions which *must* also be addressed in the case of QCD. In addition, one of the results of our analysis will be a possible method for unravelling duality violations in QCD itself.

The model starts from the $\Pi_{VV} - \Pi_{AA}$ vacuum polarization Green's function, in the chiral limit, given in terms of a spectrum consisting of two infinite towers of equally-spaced meson resonances, together with the rho meson and the massless pion, which are treated separately. Similar models can be found, e.g., in refs. [7, 9 − 12].

The fact that the spectrum is infinite is crucial and underlies all the interesting properties to be discussed. This infiniteness of the spectrum is deeply rooted in the $1/N_c$ expansion of QCD. In fact, as a first step, we will take the large-N_c limit and consider a spectrum of resonances with vanishing width. This has the advantage that all quantities can be analytically calculated. As a second step, following ref. [7], we will give the resonances a width as a subleading $1/N_c$ effect, while making sure that known analytical properties of the Green's function are not spoiled. We will thus be able to study a rather realistic model, allowing us to draw some conclusions on the issue of duality violations in the real world.

It is obvious that, in order for eq. (1.1) to be useful, an assumption has to be made. If the asymptotic regime starts at a value of q^2 which is higher than the s_0 employed in this equation, the use of the approximate expansion $\Pi_{OPE}(q^2)$ will completely miss all the physics of the full function $\Pi(q^2)$, resulting in so large an error that, in fact, the approximation will become totally invalid [13]. In the case of our model the asymptotic regime can only start after the contribution of the two towers of resonances has been taken into account, which means that the s_0 scale has to be larger than the two lowest-lying states in these towers. The model might overemphasize the effects of duality violations, but, by the same token, it provides a means to identify the causes of these effects.

Past experience accumulated over the years suggests that the case of real QCD may be less drastic than our model as far as the energy scale at which the OPE starts being a useful approximation is concerned. In other words, previous analyses of QCD which rely on the use of the OPE do not necessarily have to have systematic errors of the same size as those encountered in our model. But the model can be used to compare the different methods of analysis to see if there is one which is more reliable than the others.

JHEP08(2005)076

In real life, the values employed for s_0 are in the interval $\sim 1.5 - 3.0$ GeV^2 and the lore is that this is expected to be high enough for the OPE to set in. The agreement within present errors in the determination of α_s from tau decays [5] with those from other determinations at much larger energy scales [14] can be taken as a confirmation of this. However, a much more accurate extraction in a new generation of precision experiments might show discrepancies between the different methods of analysis. In fact, there is already a glimpse of trouble in the determination of quark masses [15], which becomes a more serious discrepancy in the terms which appear at higher order in the OPE, such as condensates [16].[2] We expect the lessons on duality violations we learn from our model to be of help in all these circumstances.

2. Duality violations in the large-N_c limit

We will concentrate on the two-point functions of vector and axial-vector currents

$$\Pi^{V,A}_{\mu\nu}(q) = i \int d^4x\, e^{iqx} \langle J^{V,A}_{\mu}(x) J^{\dagger\ V,A}_{\nu}(0)\rangle = \left(q_\mu q_\nu - g_{\mu\nu} q^2\right) \Pi_{V,A}(q^2)\,, \tag{2.1}$$

where, for definiteness, $J^\mu_V(x) = \overline{d}(x)\gamma^\mu u(x)$ and $J^\mu_A(x) = \overline{d}(x)\gamma^\mu\gamma^5 u(x)$. Throughout the paper, we will stay in the chiral limit for simplicity. Both functions, $\Pi_{V,A}(q^2)$ in eq. (2.1) satisfy the dispersion relation

$$\Pi_{V,A}(q^2) = \int_0^\infty \frac{dt}{t - q^2 - i\epsilon}\, \frac{1}{\pi}\, \mathrm{Im}\, \Pi_{V,A}(t)\,, \tag{2.2}$$

up to one subtraction.

According to the discussion in the introduction, and following refs. [7, 9], we will assume the following spectra:

$$\begin{aligned} \frac{1}{\pi}\, \mathrm{Im}\, \Pi_V(t) &= 2F_\rho^2 \delta(t - M_\rho^2) + 2\sum_{n=0}^{\infty} F_V^2(n)\delta(t - M_V^2(n))\,, \\ \frac{1}{\pi}\, \mathrm{Im}\, \Pi_A(t) &= 2F_0^2 \delta(t) + 2\sum_{n=0}^{\infty} F_A^2(n)\delta(t - M_A^2(n))\,. \end{aligned} \tag{2.3}$$

Here F_ρ is the electromagnetic decay constant of the ρ, and M_ρ is its mass. $F_{V,A}(n)$ are the electromagnetic decay constants of resonance n in the vector and axial channels, while $M_{V,A}(n)$ are the corresponding masses. F_0 is the pion decay constant in the chiral limit. The dependence on the resonance index n is taken as follows:

$$F^2_{V,A}(n) = F^2 = \text{constant}\,, \qquad M^2_{V,A}(n) = m^2_{V,A} + n\Lambda^2\,, \tag{2.4}$$

which is compatible with known properties of the large-N_c limit of QCD [6], as well as properties of the associated Regge theory [19].

[2] For a nice summary of results, see table 1 in ref. [17]. Since certain electroweak matrix elements are related to condensates [2], one can also infer the latter from lattice determinations of the former. See table 8 in ref. [18].

The combination

$$\Pi(q^2) = \frac{1}{2}(\Pi_V(q^2) - \Pi_A(q^2)) \tag{2.5}$$

thus reads

$$\Pi(q^2) = \frac{F_0^2}{q^2} + \frac{F_\rho^2}{-q^2 + M_\rho^2} - \sum_{n=0}^{\infty} \frac{F^2}{-q^2 + M_A^2(n)} + \sum_{n=0}^{\infty} \frac{F^2}{-q^2 + M_V^2(n)} \,. \tag{2.6}$$

Note that the upper end of the integration region in eq. (2.2) requires the introduction of a cutoff, $\Lambda_{\rm CO}$, to render the integrals well defined. This cutoff must satisfy chiral symmetry in order not to introduce any explicit breaking through the regulator. This is accomplished by demanding that $\Lambda_{\rm CO}^2 \sim N_V \Lambda^2 \sim N_A \Lambda^2$ as $N_{V,A} \to \infty$. Of course, physical results are independent of the precise details as to how this limit is taken, in agreement with very general properties of field theory [10].

One can see this explicitly in eq. (2.6). The infinite sums are by itself divergent and have to be regularized. In order to obtain a convergent result, one has to choose the same regulator for both axial and vector towers, i.e. $N_V = N_A$, in this case. Infinities then cancel and the two-point function can be expressed in terms of the Digamma function with the use of the identity

$$\lim_{N\to\infty} \left\{ \sum_{n=1}^{N} \frac{1}{z+n} - \sum_{n=1}^{N} \frac{1}{n} \right\} = -\psi(z) - \frac{1}{z} - \gamma_E \,, \tag{2.7}$$

where γ_E is the Euler-Mascheroni constant and $\psi(z)$ is the Digamma function, defined as

$$\psi(z) = \int_0^\infty \left(\frac{e^{-t}}{t} - \frac{e^{-zt}}{1 - e^{-t}} \right) dt = \frac{d}{dz} \log \Gamma(z) \,. \tag{2.8}$$

Thus, it follows that

$$\Pi(q^2) = \frac{F_0^2}{q^2} + \frac{F_\rho^2}{-q^2 + M_\rho^2} + \frac{F^2}{\Lambda^2} \left[\psi \left(\frac{-q^2 + m_A^2}{\Lambda^2} \right) - \psi \left(\frac{-q^2 + m_V^2}{\Lambda^2} \right) \right] . \tag{2.9}$$

Furthermore, we will impose the following conditions on our model:

$$\frac{2}{3} \frac{N_c}{16\pi^2} = \frac{F^2}{\Lambda^2} \,, \tag{2.10}$$

so that the coefficient of the parton-model logarithm is given by a free-quark loop;

$$F_\rho^2 = F^2 \left(\frac{m_V^2}{\Lambda^2} - \frac{1}{2} \right) , \qquad F_0^2 = F^2 \left(\frac{m_A^2}{\Lambda^2} - \frac{1}{2} \right) , \tag{2.11}$$

and

$$-2F_\rho^2 M_\rho^2 + F^2 \Lambda^2 \left(\frac{m_V^4}{\Lambda^4} - \frac{m_V^2}{\Lambda^2} + \frac{1}{6} \right) = F^2 \Lambda^2 \left(\frac{m_A^4}{\Lambda^4} - \frac{m_A^2}{\Lambda^2} + \frac{1}{6} \right) , \tag{2.12}$$

so that, as in the case of real QCD, there are effectively no dimension-two or dimension-four operators in the OPE of $\Pi(q^2)$ (see below). Note that eqs. (2.11) and (2.12) would not be consistent if $F_\rho = 0$. Since we want our model to be semi-realistic, this is the reason why

JHEP08(2005)076

we separated the rho meson from the vector tower in eq. (2.3). This is also natural from the point of view of Regge theory, as the rho-meson mass is low enough to be below the onset of Regge trajectories (presumably at a scale of $\mathcal{O}(1\ GeV)$). The a_1 is heavier and thus we include it in the axial tower.[3] At any rate, we will see that what really matters is the analytic properties of the OPE and these depend on the tower as a whole, rather than on the properties of any individual resonance.

Knowledge of the spectrum (2.3) allows us to calculate the full Green's function $\Pi(q^2)$ explicitly. Defining the spectral function $\rho(t) = (1/\pi)\,\mathrm{Im}\,\Pi(t)$ one has that (with $Q^2 = -q^2$)

$$\Pi(-Q^2) = \int_0^\infty \frac{dt}{t+Q^2-i\epsilon}\rho(t) \qquad \underset{\text{large}Q^2>0}{\Longrightarrow} \qquad \Pi_{OPE}(-Q^2) \approx \sum_{k=1,2,3,\ldots} \frac{C_{2k}}{Q^{2k}}\,, \qquad (2.13)$$

where the $1/Q^2$ expansion in the second equation above is akin to the Operator Product Expansion in QCD. Note that a naive expansion in powers of t/Q^2 under the integral sign is *not* an allowed mathematical operation. Consequently, in order to obtain the correct $1/Q^2$ expansion due care must be exercised. The correct OPE can be derived by using (the derivative of) eq. (2.8) and the expansion

$$e^{xz}\frac{z}{e^z-1} = \sum_{n=0}^{\infty} B_n(x)\frac{1}{n!}z^n\,, \qquad (2.14)$$

wherein $B_n(x)$ are the Bernoulli polynomials. In this way one arrives at the following expressions for the OPE coefficients C_{2k}:

$$C_{2k} = -F_0^2\ \delta_{k,1} + (-1)^{k+1}\left[F_\rho^2 M_\rho^{2k-2} - \frac{1}{k}F^2\Lambda^{2k-2}\left\{B_k\left(\frac{m_V^2}{\Lambda^2}\right) - B_k\left(\frac{m_A^2}{\Lambda^2}\right)\right\}\right]. \qquad (2.15)$$

In particular, the first few coefficients read[4]

$$\begin{aligned}
C_2 &= +F_\rho^2 - F_0^2 - F^2\left\{B_1\left(\frac{m_V^2}{\Lambda^2}\right) - B_1\left(\frac{m_A^2}{\Lambda^2}\right)\right\}, \\
C_4 &= -F_\rho^2 M_\rho^2 + \frac{1}{2}F^2\Lambda^2\left\{B_2\left(\frac{m_V^2}{\Lambda^2}\right) - B_2\left(\frac{m_A^2}{\Lambda^2}\right)\right\}, \\
C_6 &= +F_\rho^2 M_\rho^4 - \frac{1}{3}F^2\Lambda^4\left\{B_3\left(\frac{m_V^2}{\Lambda^2}\right) - B_3\left(\frac{m_A^2}{\Lambda^2}\right)\right\}, \\
C_8 &= -F_\rho^2 M_\rho^6 + \frac{1}{4}F^2\Lambda^6\left\{B_4\left(\frac{m_V^2}{\Lambda^2}\right) - B_4\left(\frac{m_A^2}{\Lambda^2}\right)\right\}, \qquad (2.16)
\end{aligned}$$

and the first few Bernoulli polynomials are

$$\begin{aligned}
&B_0(x) = 1\,, \qquad B_1(x) = x - \frac{1}{2}\,, \qquad B_2(x) = x^2 - x + \frac{1}{6}\,, \\
&B_3(x) = x^3 - \frac{3}{2}x^2 + \frac{1}{2}x\,, \qquad B_4(x) = x^4 - 2x^3 + x^2 - \frac{1}{30}\,. \qquad (2.17)
\end{aligned}$$

[3] We could also have separated the a_1, but that would introduce unnecessary free parameters without any crucial change in the analytic properties of the OPE.

[4] In fact, $C_{2,4}$ vanish identically because of the conditions (2.10), (2.12).

As already stated, the OPE cannot be obtained by naively expanding at large Q^2 under the integral sign in eq. (2.13). We emphasize that this feature is not specific to our model and is, in fact, also true in QCD. Note that, if a naive $1/Q^2$ expansion were valid in QCD, there could be no $\log Q^2$ dependence in C_{2k} and all anomalous dimensions would have to vanish, which is obviously not the case. Our model does share with QCD the property of a non-trivial expansion in $1/Q^2$ but, in the large-N_c limit, it still misses all these log's. With the introduction of finite widths in the next section, this drawback will be somewhat ameliorated.

It thus follows from the previous discussion that the moments

$$M_n(s_0) = \int_0^{s_0} dt\ t^n \rho(t) \tag{2.18}$$

are *not* the coefficients of the OPE, C_{2k}. In order to obtain the actual relation between $M_n(s_0)$ and C_{2k}, it is convenient to first calculate the Laplace transform of the dispersion relation (2.13)

$$\Pi(-Q^2) = \int_0^{\infty} d\tau\ e^{-\tau Q^2}\ \widehat{\rho}(\tau) \qquad \text{with} \qquad \widehat{\rho}(\tau) = \int_0^{\infty} dt\ e^{-t\tau} \rho(t)\,. \tag{2.19}$$

Plugging in the $1/Q^2$ expansion of eq. (2.13) and identifying Laplace transforms on both sides, one obtains

$$\sum_{k=1}^{\infty} \frac{C_{2k}}{(k-1)!}\ \tau^{k-1} = \int_0^{\infty} dt\ e^{-t\tau} \rho(t)\,, \tag{2.20}$$

and therefore, finally,

$$C_{2k} = \lim_{\tau\to 0} \left\{ (-1)^{k-1} \int_0^{\infty} dt\ t^{k-1}\ e^{-t\tau} \rho(t) \right\}. \tag{2.21}$$

As an exercise one can use the expression (2.21) to recover our results in eq. (2.16). It is the slow fall-off with t of $\rho(t)$ which is responsible for all the complications and, in particular, the duality violations. If $\rho(t)$ were falling off faster than any power at large t, one could take the $\tau \to 0$ inside the integral, and the naive $1/Q^2$ expansion of the dispersion integral in eq. (2.13) would be valid.

In actual fact, the calculation of the moments (2.18) yields

$$\begin{aligned}
M_0(s_0) &= C_2 - F^2\Big[B_1(x_V) - B_1(x_A)\Big],\\
M_1(s_0) &= -C_4 - F^2\Big[B_1(x_V) - B_1(x_A)\Big]s_0 + \frac{1}{2}F^2\Lambda^2\Big[B_2(x_V) - B_2(x_A)\Big],\\
M_2(s_0) &= C_6 - F^2\Big[B_1(x_V) - B_1(x_A)\Big]s_0^2 + F^2\Lambda^2\Big[B_2(x_V) - B_2(x_A)\Big]s_0 -\\
&\quad -\frac{1}{3}F^2\Lambda^4\Big[B_3(x_V) - B_3(x_A)\Big],\\
M_3(s_0) &= -C_8 - F^2\Big[B_1(x_V) - B_1(x_A)\Big]s_0^3 + \frac{3}{2}F^2\Lambda^2\Big[B_2(x_V) - B_2(x_A)\Big]s_0^2 -\\
&\quad -F^2\Lambda^4\Big[B_3(x_V) - B_3(x_A)\Big]s_0 + \frac{1}{4}F^2\Lambda^6\Big[B_4(x_V) - B_4(x_A)\Big],
\end{aligned} \tag{2.22}$$

where the C_{2k} are given in eqs. (2.16), and we have defined $0 < x_{V,A} < 1$ as the fractional parts of $(s_0 - m_{V,A}^2)/\Lambda^2$, respectively. The above expressions are valid when $s_0 > m_V^2$, i.e., when both the vector and axial towers are included. In these expressions, the points $x_{V,A} = 0, 1$ should be excluded because they correspond to the singularities of the delta functions in the spectrum, cf. eq. (2.3). We have kept the coefficients $C_{2,4}$ for illustrative purposes, even though they actually vanish because of the constraints (2.10)–(2.12). Perhaps several comments to explain the pattern in the result of eq. (2.22) are in order.

First, these expressions clearly show that there is no s_0 at which the moments equal the OPE coefficients, C_{2k}, and consequently, in the world of $N_c \to \infty$ described by our model, there is no such thing as a true "duality point." There are always duality violations in the form of a polynomial in the variables $x_{V,A}$. As can be seen in figure 2, these violations are step-function "oscillations" around the corresponding OPE coefficient. Note that the OPE coefficients $C_{6,8}$ are numerically negligible (using the parameters in eq. (2.23) below) compared to the oscillations shown in figure 2 for the corresponding moments $M_{2,3}$.

Looking at eqs. (2.22), one sees that there is some recursiveness, i.e. higher moments depend on the duality violation already existing in lower moments. Also, higher moments have higher powers of s_0 modulating their duality violations, so the oscillations grow larger for higher moments. This means that the larger the s_0 at which one is computing the moments (2.18), the worse the duality violation. All this behavior is clearly shown in figure 2, where we have taken as the values for our parameters the set[5]

$$\begin{aligned}
F_0 &= 85.8\,\mathrm{MeV}\,, \qquad & F_\rho &= 133.884\,\mathrm{MeV}\,, \qquad & F &= 143.758\,\mathrm{MeV}\,, \\
M_\rho &= 0.767\,\mathrm{GeV}, \qquad & m_A &= 1.182\,\mathrm{GeV}\,, \qquad & m_V &= 1.49371\,\mathrm{GeV}\,, \\
\Lambda &= 1.2774\,\mathrm{GeV}\,. & & & &
\end{aligned} \tag{2.23}$$

Second, as we have said, the end points $x_{V,A} = 0, 1$ are to be excluded from the result shown in eq. (2.22). They correspond to the singularities of the delta functions in eq. (2.3), i.e. to the position of the meson masses, and cause the appearance of step-like discontinuities at the same location in all the moments $M_n(s_0)$. At the jump produced by, e.g., the kick of a vector resonance after the drop produced by an axial-vector one, figure 2 shows how one crosses the value of the corresponding coefficient of the OPE. However, since the slope at these points is infinite, there is no way to predict the C_{2k} coefficient from the value of the corresponding moment.

One might think that the introduction of a finite width could drastically improve the present situation at large N_c. However, this is not really true in the model. Although introducing a finite width certainly changes the slope to make it finite, it also moves the location of the duality points from one moment to the next. As we will discuss in more detail in the next section, the net result is that it is still very difficult to make accurate predictions.

[5]This choice is dictated by the fact that, when a nonvanishing width will be included in the next section, the spectral function resembles qualitatively the experimental data. See figure 5 below. This choice of parameters also satisfies eqs. (2.10)–(2.12).

JHEP08(2005)076

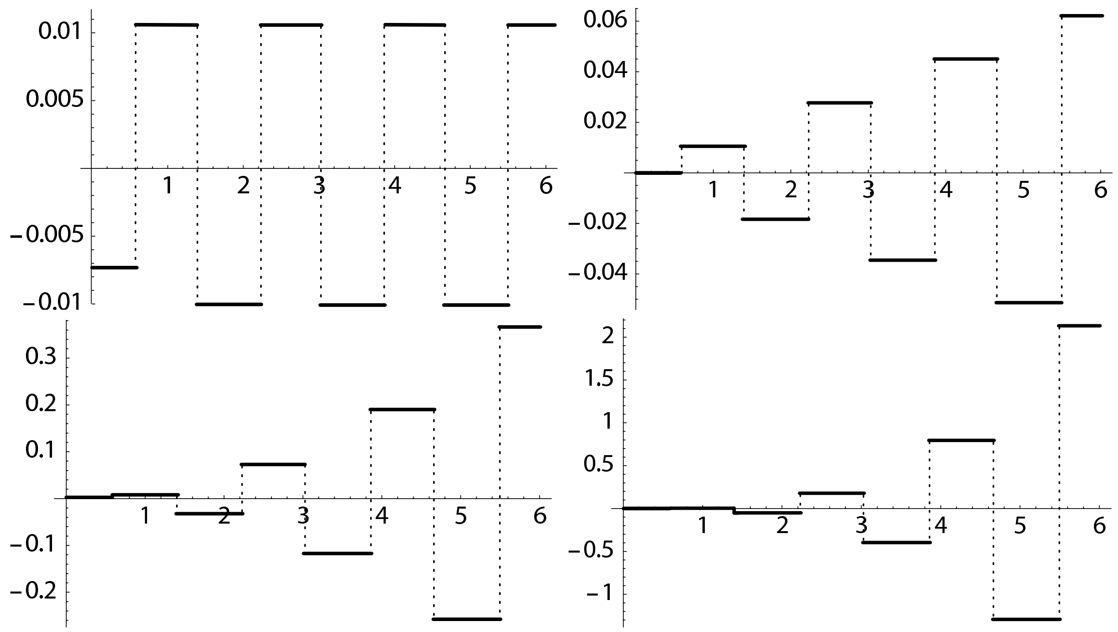

Figure 2: From left to right: M_0, M_1 (first row), M_2 and M_3 (second row), defined in eq. (2.18), as functions of the energy scale, s_0 (in GeV^2).

The best way to try to understand the relationship between the moments and the coefficients of the OPE is through the use of Cauchy's theorem, eq. (1.1). As already discussed in the introduction, the replacement $\Pi(q^2) \to \Pi_{OPE}(q^2)$ would be valid if the OPE were a convergent expansion with a radius of convergence including the circumference $|q^2| = s_0$. However, in QCD the OPE is not a convergent expansion anywhere on the $\mathrm{Re}\, q^2 > 0$ axis. Since this crucial property is shared by our model, we can now use the model to study how eq. (1.1) should be modified when the expansion $\Pi_{OPE}(q^2)$ is used instead of the exact function, $\Pi(q^2)$.

To this end, let us define $\mathcal{D}^{[n]}(s_0)$ from the equation

$$\int_0^{s_0} dt\ t^n\ \rho(t) = -\frac{1}{2\pi i} \oint_{|q^2|=s_0} dq^2\ q^{2n} \Pi_{OPE}(q^2) + \mathcal{D}^{[n]}(s_0)\,. \tag{2.24}$$

Obviously, the term $\mathcal{D}^{[n]}(s_0)$ measures the amount of duality violation and we would like to obtain a more explicit expression for it in our model.

In order to do this, note that the OPE in our model is related to the large $|z|$ expansion of the Digamma function,

$$\psi(z) \sim \log z - \frac{1}{2z} - \sum_{n=1}^{\infty} \frac{B_{2n}}{2n\ z^{2n}}\,, \qquad |\arg(z)| < \pi\,, \tag{2.25}$$

which is not a valid expansion on the negative real axis in the complex z plane. We may, nevertheless, obtain a valid expansion in this region if we use the "reflection" property of the Digamma function

$$\psi(z) = \psi(-z) - \pi \cot(\pi z) - \frac{1}{z}\,, \tag{2.26}$$

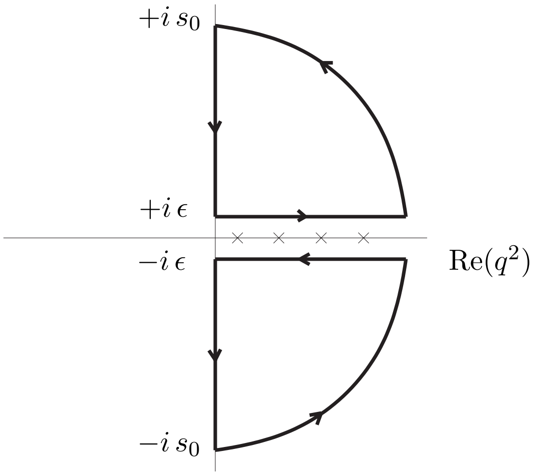

Figure 3: Contour used for the definition of the functions $\mathcal{D}^{[n]}_{\rm oscill.}(s_0)$ and $\mathcal{D}^{[n]}_{\rm const.}(s_0)$ in eqs. (2.31), (2.32).

which is valid for any complex number z. Using eq. (2.26), the appropriate expansions for large values of $|q^2|$ in the whole q^2 plane then read

$$\Pi(q^2) \approx \begin{cases} \Pi_{OPE}(q^2) + \mathcal{O}\left(e^{-2\pi|q^2|/\Lambda^2}\right), & \mathrm{Re}\, q^2 \leq 0\,; \\ \Pi_{OPE}(q^2) + \Delta_\infty(q^2) + \mathcal{O}\left(e^{-2\pi|q^2|/\Lambda^2}\right), & \mathrm{Re}\, q^2 \geq 0\,, \end{cases} \tag{2.27}$$

where

$$\Delta_\infty(q^2) = \frac{\pi F^2}{\Lambda^2}\left\{\cot\left[\pi\frac{-q^2+m_V^2}{\Lambda^2}\right] - \cot\left[\pi\frac{-q^2+m_A^2}{\Lambda^2}\right]\right\}, \tag{2.28}$$

and the subscript "∞" refers to the $N_c \to \infty$ limit. Let us emphasize again that the appearance of $\Delta_\infty(q^2)$ in eq. (2.27) gives rise to a violation of duality which does *not* go away as $|q^2| \to \infty$ (in particular it contains simple poles on the positive real axis in the q^2 plane). This duality violation comes on top of the expected exponentially suppressed contributions, which we have exhibited explicitly in eq. (2.27), and which originate from the fact that the OPE, in those regions where it is valid, is only an asymptotic expansion.[6]

Consequently, up to an exponentially small contribution, the duality violation $\mathcal{D}$ term can be written as an integral over the semicircle $|q^2| = s_0$ with $\mathrm{Re}\, q^2 \geq 0$ (taken counterclockwise) of the function $\Delta_\infty(q^2)$,

$$\mathcal{D}^{[n]}(s_0) = -\frac{1}{2\pi i}\int_{\substack{|q^2|=s_0 \\ \mathrm{Re}\, q^2 \geq 0}} dq^2\, q^{2n}\, \Delta_\infty(q^2) + \mathcal{O}\left(e^{-2\pi s_0/\Lambda^2}\right). \tag{2.29}$$

Furthermore, eq. (2.29) can be rewritten in the form of a spectral integral in the following way. The integral over the contour in figure 3 vanishes, since it encloses no singularity. It follows that the duality violation function $\mathcal{D}^{[n]}(s_0)$ in eq. (2.29) can also be expressed, up to exponentially small terms $\mathcal{O}(e^{-2\pi s_0/\Lambda^2})$, as

$$\mathcal{D}^{[n]}(s_0) = \mathcal{D}^{[n]}_{\rm oscill.}(s_0) + \mathcal{D}^{[n]}_{\rm const.}(s_0)\,, \tag{2.30}$$

[6]See the appendix.

with

$$\mathcal{D}^{[n]}_{\text{oscill.}}(s_0) = \int_0^{s_0} dt\ t^n \frac{1}{\pi} \operatorname{Im}\Delta_\infty(t+i\varepsilon) \tag{2.31}$$

$$\mathcal{D}^{[n]}_{\text{const.}}(s_0) = -\frac{1}{2\pi i}\left\{\int_{-is_0}^{-i\epsilon} + \int_{i\epsilon}^{is_0}\right\} dq^2\ q^{2n}\ \Delta_\infty(q^2)\,. \tag{2.32}$$

In these expressions, the integral (2.31) is taken over the positive real axis, in the complex q^2 plane, whereas the integrals (2.32) are taken over the imaginary axis (with $\epsilon \to 0^+$). We see that expression (2.31) is of the form of a spectral integral, just like the left-hand side of eq. (2.24). In fact, for $N_c \to \infty$, $\operatorname{Im}\Delta_\infty(q^2+i\varepsilon)$ is also a sum of delta functions with poles precisely located according to the spectrum given by the towers of eqs. (2.4). This follows from the expansion for the cotangent,

$$\pi \cot(\pi z) = \frac{1}{z} + 2z \sum_{n=1}^{\infty} \frac{1}{z^2-n^2}\,. \tag{2.33}$$

Physically, the function $\mathcal{D}^{[n]}_{\text{oscill.}}(s_0)$ is responsible for balancing all the oscillations which are present in the spectral integral on the left-hand side of eq. (2.24) but which are missed by the contour integral of the OPE on the right-hand side. The function $\mathcal{D}^{[n]}_{\text{const.}}(s_0)$, on the other hand, does not have any oscillating component, and is dominated by the region of small q^2, decaying exponentially fast in s_0 to a constant. One has

$$\mathcal{D}^{[n]}_{\text{const.}}(s_0) = \mathcal{C}^{[n]}_\infty + \mathcal{O}\left(e^{-2\pi s_0/\Lambda^2}\right), \tag{2.34}$$

with, in our $N_c = \infty$ model,[7]

$$\mathcal{C}^{[n]}_\infty = \frac{F^2\Lambda^{2n}}{n+1}\left\{B_{n+1}\left(\frac{m_V^2}{\Lambda^2}\right) - B_{n+1}\left(\frac{m_A^2}{\Lambda^2}\right)\right\} - F^2\left(m_V^2-\Lambda^2\right)^n. \tag{2.35}$$

Using this result for $n = 0,1,2,3$ in eq. (2.32) together with eqs. (2.31), (2.30) and (2.24) one may recover the results of eq. (2.22) for the moments $M_{0,1,2,3}$. Again, the total contribution to $\mathcal{D}^{[n]}(s_0)$ in eq. (2.24) does not vanish, even in the $s_0 \to \infty$ limit.

Since duality violations are caused by the lack of convergence near the positive real axis in the q^2 plane, a possible strategy to eliminate them might be to use suitable polynomials $P(t)$ in eq. (2.24) which suppress the contribution precisely from this region in q^2 by having a zero at $q^2 = s_0$. Such polynomials have been referred to as "pinched weights" in ref. [20].

This is confirmed by our large-N_c model, and it is related to the recursiveness present in the different moments in eq. (2.22). For instance, a pinched weight of the form $(1-t/s_0)$ automatically cancels the duality violating oscillation proportional to $B_1(x_V) - B_1(x_A)$ between the moments M_0 and M_1. The cancelation, however, is not complete and this pinched weight leaves behind an oscillation proportional to $[B_2(x_V) - B_2(x_A)]/s_0$ which, although suppressed at high s_0, does not vanish completely.

One can actually exploit this feature a little further and, by inspection of eq. (2.22), one easily sees that $P_3 = (1-t/s_0)^3$ is the pinched weight which best suppresses the

[7] In order to obtain this result, note that in our model $1 < \frac{m_V^2}{\Lambda^2} < 2$, whereas $\frac{m_A^2}{\Lambda^2} < 1$, cf. eq. (2.23).

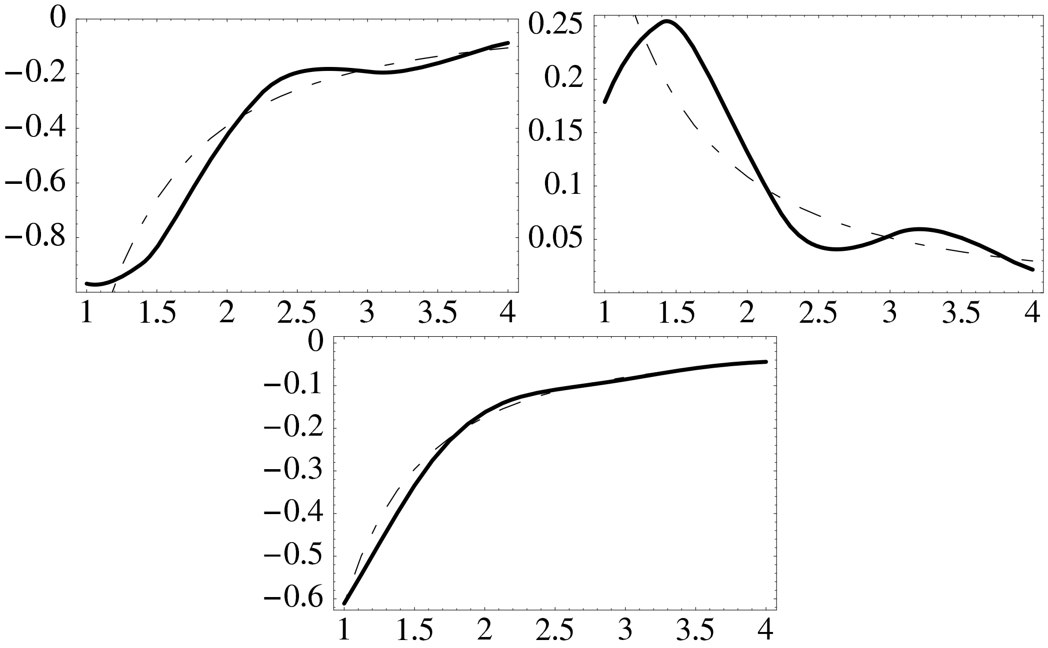

Figure 4: Integrals of the pinched weights, $\int_0^{s_0} dt\, P_{1,2,3}(t)\rho(t)$ defined in the text (solid lines, from left to right and top to bottom) and the corresponding OPE prediction (dashed lines) as a function of s_0 (in GeV^2). These integrals are expressed in units of 10^{-2} GeV^2.

duality violating oscillations among the moments $M_{0,1,2,3}$ since it only leaves behind a term proportional to $[B_4(x_V) - B_4(x_A)]/s_0^3$. This is illustrated in figure 4, where it is shown how much of a reduction in the oscillations of the left-hand side of eq. (2.24) is achieved by the pinched weight P_3 in comparison with other pinched weights previously proposed in the literature [20], i.e. $P_1 = (1-3t/s_0)(1-t/s_0)^2$ and $P_2 = (t/s_0)(1-t/s_0)^2$.

Figure 4 also shows that the OPE curve more or less interpolates through the oscillations in the spectral integral. As one can see, there are points at which the oscillation happens to cross the OPE curve so that, at these points, all duality violations effectively vanish. Based on this, one could imagine guessing the OPE coefficients by some sort of averaging over one full oscillation. Regretfully, this behavior sensitively depends on the fact that we are considering the $N_c \to \infty$ limit. The inclusion of a finite width essentially wipes out any oscillating signal and one is left without any clue as to where to take the average.

In the next section we will discuss in detail the inclusion of a finite width as well as those features which survive the passage to this more realistic setting.

3. Duality violations at finite N_c

Since the issue of duality violations hinges strongly on the analytic properties of the OPE and the corresponding Green's functions, it is clear that the introduction of a finite width has to be done with some care in order not to spoil these analytic properties.

JHEP08(2005)076

Moreover, in QCD finite widths appear as a consequence of subleading effects in the $1/N_c$ expansion. It is clear that if one knew how to properly include all these $1/N_c$ effects, one would incorporate just the right $1/N_c$ corrections to give resonances a finite width, while at the same time preserving the relevant analytic properties of $\Pi(q^2)$. Among those properties, the most important one for us will be the existence of a cut in the complex plane only for $\mathrm{Re}\, q^2 > 0$. A simple Breit-Wigner function, for instance, is not good enough.

However, the solution of QCD in the large-N_c limit is unknown, let alone the $1/N_c$ corrections, so it is clear that one has to model these effects in some simple way in order to make progress. This is what has been done in ref. [7]. The hope is that the conclusions drawn from such a model will not depend in any crucial way on the particular details but rather on the generic properties of the model.

With this philosophy in mind we follow ref. [7] and introduce a subleading $1/N_c$ width, writing the vacuum polarization $\Pi(q^2)$ as

$$\Pi(q^2) = \left(1 - \frac{a}{\pi N_c}\right)^{-1} \left\{ -\frac{F_0^2}{z} + \frac{F_\rho^2}{z + M_\rho^2} - \sum_{n=0}^{\infty} \frac{F^2}{z + M_A^2(n)} + \sum_{n=0}^{\infty} \frac{F^2}{z + M_V^2(n)} \right\}, \qquad (3.1)$$

where now the variable z denotes the combination

$$z = \Lambda^2 \left(\frac{-q^2 - i\epsilon}{\Lambda^2} \right)^{\zeta}, \qquad \zeta = 1 - \frac{a}{\pi N_c}, \qquad (3.2)$$

and $M_{V,A}(n)$ are given in eq. (2.4). As in the zero-width case, the infinite sums can be expressed in terms of the Digamma function, and one obtains

$$\Pi(q^2) = \frac{1}{\zeta} \left\{ -\frac{F_0^2}{z} + \frac{F_\rho^2}{z + M_\rho^2} + \frac{F^2}{\Lambda^2} \left[\psi\left(\frac{z + m_A^2}{\Lambda^2} \right) - \psi\left(\frac{z + m_V^2}{\Lambda^2} \right) \right] \right\}. \qquad (3.3)$$

Obviously, in the $N_c \to \infty$ limit we recover the results of the previous section. The conditions of eqs. (2.10), (2.11) and (2.12) impose now the absence of any $\log z, 1/z$ and $1/z^2$ terms in the large $Q^2 = -q^2 > 0$ expansion of the Green's function $\Pi(q^2)$ in eq. (3.3).

The choice of values for the parameters in eq. (2.23) plus the choice

$$a = 0.72 \qquad (3.4)$$

for the new parameter a produces the spectral function which is plotted in figure 5. As can be seen in this figure, the model is not able to reproduce the experimental data in detail, but the qualitative agreement is good enough for our purposes. We remind the reader that our model is not meant to extract physical parameters, but only as a laboratory for testing different methods which are currently in use for the determination of the coefficients of the OPE from the data.

In the limit $N_c \to \infty$ one recovers for $\mathrm{Im}\,\Pi(q^2)$ the result with Dirac deltas of the previous section, eq. (2.3). However, at small but finite a/N_c, the dependence of every resonance propagator on q^2 through the new variable z produces a complex pole with an imaginary part, and thus a width $\Gamma_{V,A}(n)$ given by

$$\Gamma_{V,A}(n) = \frac{a}{N_c} M_{V,A}(n) \left(1 + \mathcal{O}\left(\frac{a}{N_c} \right) \right), \qquad (3.5)$$

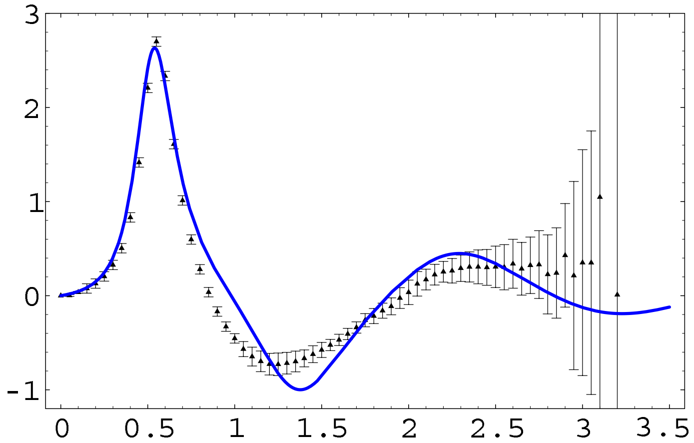

Figure 5: Comparison of the data from ALEPH and OPAL (overlaid on a single plot and including the kinematical factors of τ decay) with the model, $\frac{1}{\pi}\mathrm{Im}\Pi(q^2)$ from eq. (3.3) (solid blue line), as a function of q^2 (in GeV^2). As it is the case with the experimental data, the pion contribution, F_0^2/z in eq. (3.3) has been subtracted away.

and, mutatis mutandis, for the ρ as well. This behavior for Γ is the one expected on general grounds [7] and, as one can see, forces $\Gamma_{V,A}(n)$ to vanish as $N_c \to \infty$, although it should be noted that the width also grows with the resonance number n.

Given that the change produced by the widths amounts to the replacement (3.2), the expansion of the Green's function $\Pi(q^2)$ at large values of the momentum $|q^2|$ is similar to that in eq. (2.27):

$$\Pi(q^2) \approx \begin{cases} \Pi_{OPE}(q^2) + \mathcal{O}\left(e^{-2\pi|q^2/\Lambda^2|^\zeta}\right), & \mathrm{Re}\, q^2 \leq 0\,, \\ \Pi_{OPE}(q^2) + \Delta(q^2) + \mathcal{O}\left(e^{-2\pi|q^2/\Lambda^2|^\zeta}\right), & \mathrm{Re}\, q^2 \geq 0\,, \end{cases} \tag{3.6}$$

except that now

$$\Delta(q^2) = \frac{\pi F^2}{\Lambda^2}\,\frac{1}{\zeta}\left\{\cot\left[\pi\left(\frac{-q^2}{\Lambda^2}\right)^\zeta + \pi\frac{m_V^2}{\Lambda^2}\right] - \cot\left[\pi\left(\frac{-q^2}{\Lambda^2}\right)^\zeta + \pi\frac{m_A^2}{\Lambda^2}\right]\right\}, \tag{3.7}$$

with $\zeta = 1 - a/\pi Nc$. Similarly, the OPE is given by an expansion as in eq. (2.13) but the coefficients (2.15) are shifted by a $\log Q^2$-dependent term. For small a/N_c, the Wilson coefficients read

$$C_{2k}(Q^2)^{N_c=3} = C_{2k}^{N_c=\infty}\left(1 + \frac{a}{\pi N_c} + \frac{ka}{\pi N_c}\log\frac{Q^2}{\Lambda^2} + \mathcal{O}\left(\frac{a^2}{N_c^2}\right)\right), \tag{3.8}$$

where the $C_{2k}^{N_c=\infty}$ are those given in eq. (2.15). We will find it convenient to explicitly separate the log dependence and decompose these coefficients as [20]

$$C_{2k}(Q^2)^{N_c=3} = a_{2k} + b_{2k}\log\frac{Q^2}{\Lambda^2} + \mathcal{O}\left(\frac{a^2}{N_c^2}\right). \tag{3.9}$$

The b_{2k} would model the existence of anomalous dimensions in real QCD were it not for the fact that the latter, unlike the b_{2k}, do not vanish in the large-N_c limit. We do not consider this to be a serious drawback of the model, however, and the $1/N_c$ contributions in eq. (3.8) still mimic the $\alpha_s(m_\tau)$ contributions to the anomalous dimensions which exist in real QCD. Even though the $1/N_c$ corrections in eq. (3.8) grow larger with increasing dimension of the operator, at least for the first terms there is a sense in which the $N_c \to \infty$ limit is close to the world at $N_c = 3$ in the OPE. Plugging in our set of numbers (2.23), (3.4), the OPE coefficients are

$$\begin{aligned} a_2 &= b_2 = 0 = a_4 = b_4 \\ a_6 &= -2.8 \times 10^{-3} \mathrm{GeV}^6 \,, \qquad b_6 = -5.9 \times 10^{-4} \mathrm{GeV}^6 \,, \\ a_8 &= +1.8 \times 10^{-3} \mathrm{GeV}^8 \,, \qquad b_8 = +5.1 \times 10^{-4} \mathrm{GeV}^8 \,. \end{aligned} \tag{3.10}$$

The small $1/N_c$ correction to the Green's function $\Pi(q^2)$ in the euclidean (cf. eq. (3.8)) is in complete contradistinction to what happens to the spectral function $\mathrm{Im}\,\Pi(t)$ in the Minkowski region, $t > 0$. As emphasized in ref. [7], the reason for this is that the limits $N_c \to \infty$ and $t \to \infty$ do not commute in this region. Defining $q^2 = t > 0$, one obtains to leading order in a/N_c for the variable z of eq. (3.2) in this region,

$$z = -t\left(1 - \frac{a}{\pi N_c}\log\left(\frac{t}{\Lambda^2}\right) + i\frac{a}{N_c} + \mathcal{O}\left(\frac{a^2}{N_c^2}\right)\right) . \tag{3.11}$$

Taking imaginary parts of the reflection property for the ψ function in eq. (2.26), at large values of the momentum $t > 0$ one obtains that

$$\mathrm{Im}\,\Pi(t) = \mathrm{Im}\,\Pi_{OPE}(t) + \mathrm{Im}\,\Delta(t) \,, \tag{3.12}$$

where

$$\mathrm{Im}\,\Pi_{OPE}(t) = \frac{3a}{N_c}\,\frac{b_6}{t^3}\left(1 + \mathcal{O}\left(\frac{a}{N_c}\right)\right) + \mathcal{O}\left(\frac{1}{t^4}\right) , \tag{3.13}$$

and

$$\begin{aligned} \mathrm{Im}\,\Delta(t) = &\frac{4\pi F^2}{\Lambda^2}\; e^{-\frac{2\pi a}{N_c}\frac{t}{\Lambda^2}}\; \sin\left(\pi\frac{2t - m_A^2 - m_V^2}{\Lambda^2}\right) \sin\left(\pi\frac{m_V^2 - m_A^2}{\Lambda^2}\right)\left(1 + \mathcal{O}\left(\frac{a}{N_c}\right)\right) + \\ &+ \mathcal{O}\left(e^{-\frac{4\pi a}{N_c}\frac{t}{\Lambda^2}}\right) \,. \end{aligned} \tag{3.14}$$

The imaginary part in eq. (3.13) can be gotten from the imaginary part of the logarithm in the OPE expansion in eq. (3.8) and is also familiar from the QCD case, except for the $1/N_c$ suppression. Analogously, the cancelation of the t^{-1} and t^{-2} terms is due to the absence of the corresponding $1/Q^2$ and $1/Q^4$ terms in the OPE in the euclidean region.

The contribution shown in eq. (3.14) is completely missed by the OPE and stems from the duality-violating function $\Delta(q^2)$ in eq. (3.7). We call the reader's attention to the N_c factor in the denominator of the exponent in eq. (3.14). The expression in this equation is obtained in the large t limit when N_c is kept finite. That is to say, for finite N_c, the isolated poles of $\Delta_\infty(q^2)$ on the real axis (figure 3) become a cut. If, on the contrary, the limit $N_c \to \infty$ is taken first, then the expression (3.14) is not valid and one obtains the infinite sum of delta functions of the previous section instead. It follows that the two limits

$N_c \to \infty$ and $t \to \infty$ do not commute in the Minkowski region. We expect this effect to be quite generic, and we thus believe the exponentially damped oscillation shown in eq. (3.14) to be more general than our particular model [7].

In general, although eqs. (2.24), (2.29) are still valid, the behavior of the duality-violating function $\Delta(q^2)$ changes drastically with respect to its counterpart $\Delta_\infty(q^2)$, showing an exponential fall-off at large $|q^2|$ on the half plane $\mathrm{Re}\, q^2 \geq 0$. One has now that

$$\Delta(q^2) \underset{|q^2|\,\mathrm{large}}{\sim} e^{-2\pi \, {\frac{|q^2|}{\Lambda^2}}^{\zeta} \left|\sin\left\{\zeta(\varphi-\pi)\right\}\right|}\,, \qquad q^2 = |q^2|\, e^{i\varphi}\,, \qquad \begin{cases} 0 \leq \varphi \leq \frac{\pi}{2} \\ \dfrac{3\pi}{2} \leq \varphi \leq 2\pi \end{cases} \tag{3.15}$$

We see in particular that the limit $N_c \to \infty$ (i.e. $\zeta \to 1$) makes the values $\varphi = 0,\ 2\pi$ exceptional: when $N_c = \infty$, the exponential fall-off on the real axis completely disappears. This is of course consistent with eq. (3.14).

The exponential fall-off exhibited in eq. (3.15) implies now that the function $\mathcal{D}^{[n]}(s_0)$ vanishes exponentially at large s_0 as

$$\mathcal{D}^{[n]}(s_0) \sim \mathcal{O}\left(e^{-\frac{2\pi a}{N_c}\frac{s_0}{\Lambda^2}}\right). \tag{3.16}$$

Again we note the singular limit $N_c \to \infty$ in this expression: in the previous section we saw that $\mathcal{D}^{[n]}(s_0) \to$ "undamped oscillations," if the limit $N_c \to \infty$ is taken before s_0 is taken to infinity.

For finite N_c, one has

$$\begin{aligned} \mathcal{D}^{[n]}(s_0) &= \mathcal{D}^{[n]}_{\mathrm{oscill.}}(s_0) + \mathcal{D}^{[n]}_{\mathrm{const.}}(s_0) \underset{s_0\,\mathrm{large}}{\sim} \mathcal{O}\left(e^{-\frac{2\pi a}{N_c}\frac{s_0}{\Lambda^2}}\right), & (3.17)\\ \mathcal{D}^{[n]}_{\mathrm{oscill.}}(s_0) &= \int_0^{s_0} dt\, t^n \frac{1}{\pi}\, \mathrm{Im}\,\Delta(t+i\varepsilon) \underset{s_0\,\mathrm{large}}{\sim} -\mathcal{C}^{[n]} + \mathcal{O}\left(e^{-\frac{2\pi a}{N_c}\frac{s_0}{\Lambda^2}}\right), & (3.18)\\ \mathcal{D}^{[n]}_{\mathrm{const.}}(s_0) &= \mathcal{C}^{[n]} + \mathcal{O}\left(e^{-2\pi\frac{s_0}{\Lambda^2}}\right). & (3.19) \end{aligned}$$

We are using the hierarchy

$$e^{-\frac{2\pi a}{N_c}\frac{s_0}{\Lambda^2}} \gg e^{-2\pi\frac{s_0}{\Lambda^2}}\,, \tag{3.20}$$

which is very well satisfied for large values of s_0. Note the more stringent bound on the corrections to eq. (3.19), which results from the fact that $\mathcal{D}^{[n]}_{\mathrm{const.}}(s_0)$ is defined as an integral over $\Delta(q^2)$ for values of q^2 far away from the positive real axis.[8]

Combining eqs. (3.17)–(3.19) in the $s_0 \to \infty$ limit, it follows that

$$\mathcal{C}^{[n]} = -\int_0^\infty dt\, t^n \frac{1}{\pi}\, \mathrm{Im}\,\Delta(t+i\varepsilon)\,, \tag{3.21}$$

and, inserting this result into eq. (3.17), we obtain

$$\mathcal{D}^{[n]}(s_0) = -\int_{s_0}^\infty dt\, t^n \frac{1}{\pi}\, \mathrm{Im}\,\Delta(t+i\varepsilon) + \mathcal{O}\left(e^{-\frac{2\pi s_0}{\Lambda^2}}\right) \tag{3.22}$$

as the final expression in the finite width case, for the duality violations in eq. (2.24). Since $\mathrm{Im}\,\Delta(t+i\varepsilon) \sim \mathcal{O}(e^{-\frac{2\pi a}{N_c}\frac{t}{\Lambda^2}})$ (cf. eq. (3.14)), the integral in eq. (3.22) is indeed of order $e^{-\frac{2\pi s_0}{N_c \Lambda^2}}$, in agreement with eq. (3.17).

[8] See the appendix for the derivation of eq. (3.19).

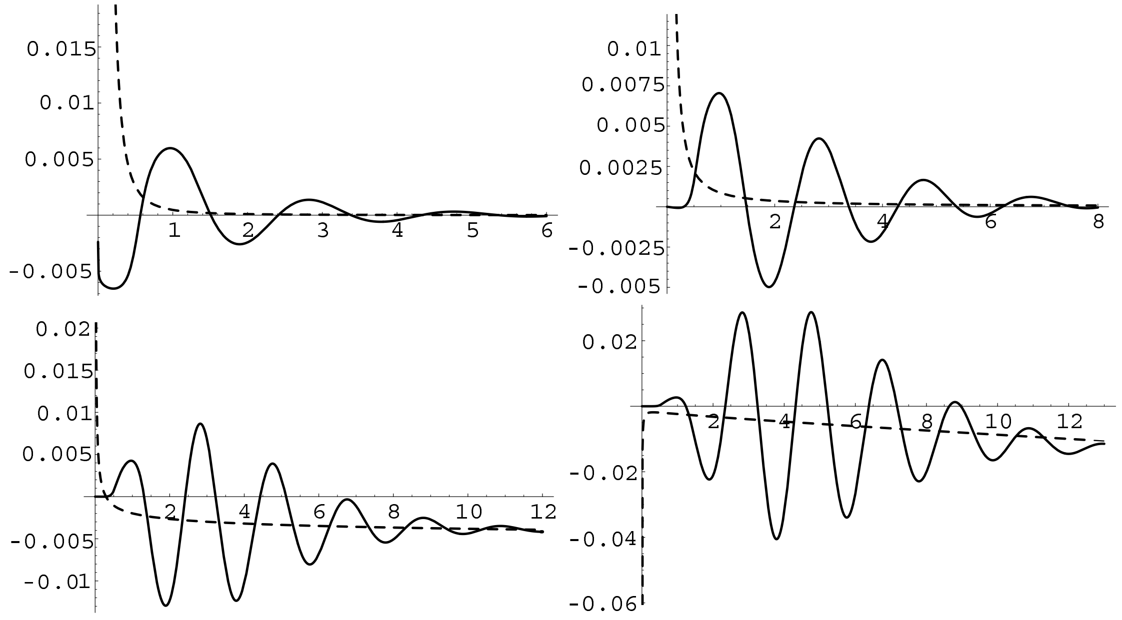

Figure 6: From left to right: M_0, M_1 (solid curves, first row), M_2 and M_3 (solid curves, second row), defined in eq. (2.18), together with the OPE prediction (dashed curves) as given by the corresponding terms in squared brackets in eqs. (3.23)–(3.26), as functions of the energy scale, s_0 (in GeV^2).

Returning to eq. (2.24), we obtain for the OPE coefficients the following set of equations:

$$\int_0^{s_0} dt\,\rho(t) + \left[\frac{b_6}{2s_0^2} - \frac{b_8}{3s_0^3} + \cdots\right] = \mathcal{D}^{[0]}(s_0) \qquad (3.23)$$

$$\int_0^{s_0} dt\,t\rho(t) + \left[\frac{b_6}{s_0} - \frac{b_8}{2s_0^2} + \cdots\right] = \mathcal{D}^{[1]}(s_0) \qquad (3.24)$$

$$\int_0^{s_0} dt\,t^2\rho(t) - \left[a_6 + b_6\log\frac{s_0}{\Lambda^2} + \frac{b_8}{s_0} + \cdots\right] = \mathcal{D}^{[2]}(s_0) \qquad (3.25)$$

$$\int_0^{s_0} dt\,t^3\rho(t) + \left[a_8 + b_8\log\frac{s_0}{\Lambda^2} - b_6 s_0 + \frac{b_{10}}{s_0} + \cdots\right] = \mathcal{D}^{[3]}(s_0) \qquad (3.26)$$

$$\vdots$$

$$\int_0^{s_0} dt\,t^7\rho(t) + \left[a_{16} + b_{16}\log\frac{s_0}{\Lambda^2} - \frac{b_6 s_0^5}{5} + \frac{b_8 s_0^4}{4} + \cdots + \frac{b_{18}}{s_0} + \cdots\right] = \mathcal{D}^{[7]}(s_0)\,, \qquad (3.27)$$

where the right-hand side is given by eq. (3.22). The results for the lowest moments (2.18) and the corresponding OPE (the terms explicitly shown in squared brackets in eqs. (3.23)–(3.26)) are plotted in figure 6.

We draw the following conclusions from eqs. (3.23)–(3.27): first, it is clear that the b coefficients of the OPE also contribute to these equations. The pattern is simple and governed by dimensional analysis: a higher order b contributes to the equation determining a lower order a accompanied by inverse powers of the scale s_0. On the other hand, a lower order b contributes to the equation determining a higher order a accompanied by *positive* powers of s_0.

Even though in real QCD the b coefficients are order α_s effects with respect to the a's, the fact that they may appear multiplied by positive powers of s_0 tells us that, in general, it is safer not to neglect them from the start, unlike what is done at present in common practice. A possible exception is the term b_6, which is the only one which has been calculated [21] and which seems to be small enough to be safely disregarded. Since this term is the only one accompanied by positive powers of s_0 in eqs. (3.23)–(3.26), it might not be too unreasonable to neglect the b terms in these equations in a first approximation. However, for higher moments, this practice may be dangerous. Notice that an s_0^4 term amounts to a factor of almost 100 GeV^8 for $s_0 = m_\tau^2 = 3.15\ \mathrm{GeV}^2$ so that, for instance, the term $b_8 s_0^4$ in the last eq. (3.27) might not be negligible even if b_8 is small.

Second, and most important, the right-hand sides of eqs. (3.23)–(3.27) do not vanish in general, except in the limit $s_0 \to \infty$. As it is obvious from these equations, the $\mathcal{D}$ terms may potentially pollute the extraction of the OPE coefficients. Consequently, in any precise determination of OPE coefficients it is unavoidable to take this duality violation into account.

In order to further appreciate this point, let us close our eyes, neglect the duality violations $\mathcal{D}$ altogether, and apply the different methods which have been employed in the literature so far.

For instance, let us start with finite-energy sum rules. The method consists in determining a duality point s_0^* from the condition $M_{0,1}(s_0^*) \simeq 0$, which is then to be used in $M_{2,3}(s_0^*)$ to predict the combinations appearing in eqs. (3.25), (3.26), namely

$$\begin{aligned} A_6(s_0^*) &\equiv a_6 + b_6 \log \frac{s_0^*}{\Lambda^2} + \frac{b_8}{s_0^*} + \cdots , \\ A_8(s_0^*) &\equiv a_8 + b_8 \log \frac{s_0^*}{\Lambda^2} - b_6 s_0^* + \frac{b_{10}}{s_0^*} + \cdots \end{aligned} \tag{3.28}$$

In our model the first duality point happens to sit at $s_0^* = 1.472\ \mathrm{GeV}^2$, yielding the predictions

$$A_6^{FESR} = -4.9 \cdot 10^{-3}\,\mathrm{GeV}^6 , \qquad A_8^{FESR} = +9.3 \cdot 10^{-3}\,\mathrm{GeV}^8 , \tag{3.29}$$

which can be compared to the correct values

$$A_6(1.472\ \mathrm{GeV}^2) = -2.4 \cdot 10^{-3}\mathrm{GeV}^6 , \quad A_8(1.472\ \mathrm{GeV}^2) = +2.6 \cdot 10^{-3}\mathrm{GeV}^8 . \tag{3.30}$$

There is a second duality point around 2.4 GeV^2 fulfilling either $M_0(s_0^*) = 0$ or $M_1(s_0^*) = 0$, but not both. Choosing the one which satisfies $M_1(s_0^*) = 0$, for instance, one gets $s_0^* = 2.363\ \mathrm{GeV}^2$ and this yields

$$A_6^{FESR} = -2.0 \cdot 10^{-3}\,\mathrm{GeV}^6 , \qquad A_8^{FESR} = -1.6 \cdot 10^{-3}\,\mathrm{GeV}^8 , \tag{3.31}$$

to be compared to

$$A_6(2.363\,\mathrm{GeV}^2) = -2.8 \cdot 10^{-3}\mathrm{GeV}^6 , \qquad A_8(2.363\,\mathrm{GeV}^2) = +3.4 \cdot 10^{-3}\mathrm{GeV}^8 . \tag{3.32}$$

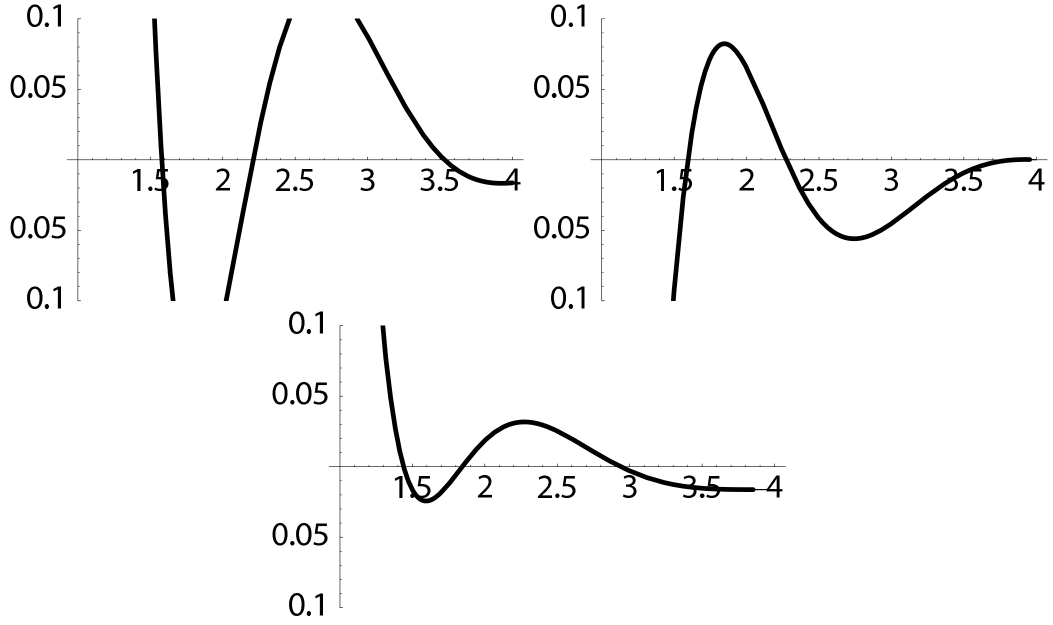

Figure 7: Difference between the integrals of the pinched weights, $\int_0^{s_0} dt\ P_{1,2,3}(t)\rho(t)$ and the corresponding OPE contribution from eqs. (3.23)–(3.26) (in units of 10^{-3} GeV^2), as a function of s_0 (in GeV^2), from left to right and top to bottom, respectively.

As we see, in going from the first to the second duality point, A_6 is reduced by a factor 2 and A_8 changes sign. Interestingly enough, this is precisely the trend seen in the corresponding determinations in the literature [22, 23].

From the comparison of both results (3.29) and (3.31), it seems that there is no dramatic advantage to making the prediction using the second duality point rather than the first, even though at the second point s_0 has a larger value.[9] Moreover, while going to a larger s_0 is in principle better because the duality violations $\mathcal{D}^{[n]}(s_0)$ become smaller, if this is done while keeping all the b coefficients to zero, i.e. taking the A's above as estimates for the a's, then the growth of the moments $M_{2,3}(s_0)$ with s_0 — they are actually divergent because of eq. (3.13) — is numerically absorbed by a wrong shift in $a_{6,8}$. As we see in eqs. (3.29) and (3.31), this may invalidate the advantage of choosing a larger s_0. Furthermore, in the real world the experimental error bars are much bigger at larger s_0, the QCD value of b_6 is very small and that of b_8 is unknown. This makes it difficult to know exactly what explains the difference between the results obtained in the literature using finite-energy sum rules [22, 23, 17].[10]

Let us next consider pinched weights, which have been suggested [20, 25] as a way to reduce the amount of duality violations. However, the use of pinched weights is no guarantee that one can do away with the duality violations altogether. For instance, we have followed ref. [20] and fitted the OPE coefficients to the combination of moments

[9]The prediction for A_6 at the second s_0^* is somewhat better than at the first, but this is no longer the case for A_8.

[10]Reference [24] finds numerical agreement with ref. [23] but, in fact, it does not have the second duality point the analysis of ref. [23] is based on.

obtained with the pinched weights $P_1 = (1-3t/s_0)(1-t/s_0)^2$ and $P_2 = (t/s_0)(1-t/s_0)^2$, neglecting duality violations. We have done this with 20 points in the window 1.5 GeV^2 $\leq s_0 \leq 3.5$ GeV^2. The upper end in this window was identified by noting that the tau mass roughly coincides with the mass of the $\rho(1700)$ in QCD, and in our model this resonance happens to be at $m^2_{\rho''} \simeq 3.8$ GeV^2. The result from the fit can be interpreted as some sort of average over the window in s_0 of the combinations $A_{6,8}$ in eq. (3.28), and yields

$$A_6^{\rm pinch} = -3.8 \times 10^{-3}\,{\rm GeV}^6\,, \qquad A_8^{\rm pinch} = 6.5 \times 10^{-3}\,{\rm GeV}^8\,. \tag{3.33}$$

As one can see, the error made is again rather large (particularly in the case of A_8) and, in fact, comparable to that using finite-energy sum rules in eqs. (3.29), (3.31). We did not see any clear improvement in precision by changing details of the fit such as, e.g., the window of s_0 values used.

Since pinched weights suppress duality violations, one may try to design "good" pinched weights which have as small duality violations as possible. Assuming a general expression for the duality violations of the form (cf. eq. (3.14))

$$\frac{1}{\pi}\,{\rm Im}\,\Delta(t) = \kappa\; e^{-\gamma t}\;\sin\left(\alpha + \beta t\right), \tag{3.34}$$

for certain values of the parameters κ, γ, α and β, one could ask which is the pinched weight, involving moments not higher than M_3, which minimizes the amount of duality violations. As before, the answer to this question is $P_3 = (1-t/s_0)^3$. The reason is that, given the general form in eq. (3.34), one finds that P_3's residual oscillation is damped by the factor $s_0^{-3} e^{-\gamma s_0}$, while in the case of $P_{1,2}$ the damping factor is only $s_0^{-2} e^{-\gamma s_0}$. This is a behavior reminiscent of the $N_c = \infty$ case in the previous section.[11] Figure 7 shows the difference between the integral of the pinched weights $P_{1,2,3}$ and their corresponding OPE contribution from eqs. (3.23)–(3.26) as a function of s_0. If there were no duality violations these curves should be a flat zero. As this figure shows, P_3 has the smallest duality violations.

In ref. [17] a Laplace sum rules analysis was done. Neglecting the b coefficients one obtains for the a coefficients of the OPE the equations

$$\begin{aligned} a_6^L - a_{10}^L\frac{\tau^2}{12} + \cdots &= \frac{6}{\tau^2}\int_0^{s_0} dt\, e^{-t\tau}\rho(t) + \frac{2}{\tau}\int_0^{s_0} dt\, t\; e^{-t\tau}\rho(t)\,, \\ a_8^L + a_{10}^L\frac{\tau}{2} + \cdots &= -\frac{12}{\tau^3}\int_0^{s_0} dt\, e^{-t\tau}\rho(t) - \frac{6}{\tau^2}\int_0^{s_0} dt\, t e^{-t\tau}\rho(t)\,. \end{aligned} \tag{3.35}$$

Requiring stability under variations in the Laplace variable τ one can determine $a^L_{6,8}$.[12] In figure 8 we have plotted the true values for $a_{6,8}$ from eq. (3.10) together with the τ dependence of a_6^L, a_8^L – neglecting a_{10}^L and higher. The upper limit in the Laplace integral has been chosen to be the second duality point from the previous finite-energy sum rules analysis of eq. (3.31), $s_0^* \simeq 2.35\,{\rm GeV}^2$, but there is no qualitative change if the first duality

[11] This is a general result. For moments not higher than M_n the optimal pinched weight is $(1-t/s_0)^n$ and the residual oscillation is modulated by $s_0^{-n} e^{-\gamma s_0}$.

[12] Obviously, the true a coefficients (3.10) are independent of τ.

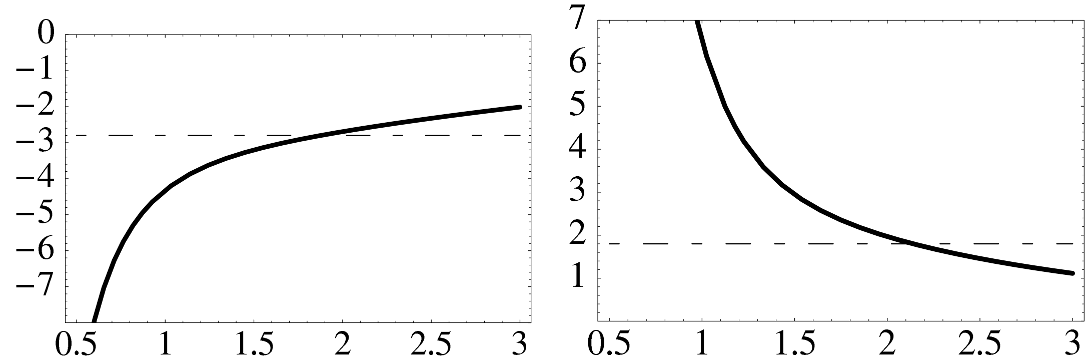

Figure 8: Plot of the coefficients a_6^L (solid curve, left) and a_8^L (solid curve, right), together with the corresponding true values $a_{6,8}$ (dashed horizontal lines) from eqs. (3.10) (all in units of 10^{-3}), as a function of the Laplace variable, τ (in GeV^{-2}).

point (3.29) is used instead. As it can be clearly seen, no sign of stability in τ is found. (We do not expect this to change qualitatively if a_{10}, b_6 etc. are included.) This is unlike what is found in QCD [17] and may be another sign of what we already said in the introduction concerning the model's tendency to maximize the violations of duality.

Finally, we also used the MHA method [26]. In this case one truncates the spectrum to a finite number of resonances whose parameters are adjusted so that the low- and high-energy expansions of the $\Pi(q^2)$ function in the large-N_c limit are reproduced. In this way one constructs an interpolator for the function $\Pi(q^2)$, called $\Pi_{MHA}(q^2)$ with which it is possible to calculate, e.g., the integrals which determine the relevant couplings governing semileptonic kaon decays. However, in the present case the situation is slightly different because one wishes to use $\Pi_{MHA}(q^2)$ to predict coefficients of the high-energy expansion, and not as an interpolator for an integrand.

The function $\Pi_{MHA}(q^2)$ is constructed as[13]

$$\Pi(q^2)^{MHA} = \frac{F_0^2}{q^2} + \frac{\widetilde{F}_V^2}{\widetilde{M}_V^2 - q^2} - \frac{\widetilde{F}_A^2}{\widetilde{M}_A^2 - q^2}\,, \tag{3.36}$$

with the parameters $\widetilde{M}_V, \widetilde{M}_A, \widetilde{F}_V, \widetilde{F}_A$ to be determined from the conditions $C_{2,4} = 0$ and the values of L_{10} and the pion electromagnetic mass difference in the large-N_c limit, as taken from the model in the previous section, eq. (2.9).

They are given by the following expressions:

$$\begin{aligned} L_{10} &= -\frac{1}{4} F_0^2 \frac{\widetilde{M}_A^2 + \widetilde{M}_V^2}{\widetilde{M}_V^2 \widetilde{M}_A^2} = -(5.2 \pm 0.5) \cdot 10^{-3} \\ m_\pi^+ - m_\pi^0 &= \left(\frac{3\alpha}{8\pi^2 m_\pi F_\pi^2} \right) F_0^2 \frac{\widetilde{M}_A^2 \widetilde{M}_V^2}{\widetilde{M}_A^2 - \widetilde{M}_V^2} \log\left(\frac{\widetilde{M}_A^2}{\widetilde{M}_V^2} \right) = (4.2 \pm 0.4) \cdot 10^{-3}\,\mathrm{GeV}\,, \end{aligned} \tag{3.37}$$

where $\alpha \simeq 1/137$ is the electromagnetic coupling constant, and the error has been estimated on account of the large-N_c approximation of the model. Equations (3.37) fix the parameters

[13] See ref. [27] for a more elaborated version of this method applied to QCD, in which also a ρ' is included.

in eq. (3.36) to be

$$\begin{aligned} \widetilde{M}_V &= 0.70 \pm 0.01\,\mathrm{GeV}\,, \qquad & \widetilde{M}_A &= 1.00 \pm 0.03\,\mathrm{GeV} \\ \widetilde{F}_V &= 122 \pm 6\,\mathrm{MeV}\,, & \widetilde{F}_A &= 84 \pm 7\,\mathrm{MeV}\,. \end{aligned} \tag{3.38}$$

Feeding expression (3.36) with these values one has a prediction for the full vacuum polarization function. In the euclidean region the prediction is very good for a broad range of intermediate values of q^2. For example, at $q^2 = -1$ GeV^2 the error between $\Pi(q^2)$ and $\Pi_{MHA}(q^2)$ is only $\sim 3\%$ [14].

Expanding eq. (3.36) in inverse powers of q^2, we obtain the following prediction for the OPE coefficients:

$$a_6^{MHA} = -(3.6 \pm 0.3) \times 10^{-3}\,\mathrm{GeV}^6\,, \qquad a_8^{MHA} = (5.4 \pm 0.7) \times 10^{-3}\,\mathrm{GeV}^8\,, \tag{3.39}$$

to be compared to the results in eq. (3.10). Again, no dramatic improvement is found as compared to previous methods. As with other methods, the prediction for a_8 is worse than that for a_6.

In summary, the errors in the determinations of OPE coefficients from the different methods tend to be large in the present model. No method can be claimed to be more precise than the others, and the error made is comparable in size to the spread of values among the different methods.

It is difficult to say what happens in the case of QCD. For a_6, the spread of values in QCD found in the literature is not as bad as in the case of our model. This could be related to the fact that the size of the coefficient b_6 relative to a_6 is much smaller in QCD than it is in the model. But also in QCD the discrepancies are clearly more serious for a_8 and higher coefficients [17].

One of the lessons from our analysis of the model is that one should not ignore duality violations represented by the $\mathcal{D}$ terms in eqs. (3.23)–(3.27). In figure 9, we have plotted these $\mathcal{D}$ terms (solid lines). As one can see, they show zeros at certain values of $s_0 \sim 1.5, 2.4, 3.4, \ldots$ GeV. These zeros correspond to values of s_0 where the duality violations vanish and they are therefore the optimal points which one would like to use as duality points in any finite-energy sum rule analysis. However, the location of these zeros is not precisely determined because, as figure 9 shows, the zeros are not universal but move from one spectral moment to the next. This is one of the reasons why the finite-energy sum rule determination of OPE coefficients in eqs. (3.28)–(3.32) has large errors. Consequently, as such duality violations are likely to be present in QCD as well, we will now use the model to show how these $\mathcal{D}$ terms may be included in a realistic analysis also in QCD.

Our basic assumption will be that our result (3.22) together with the functional form of a damped oscillation as in eq. (3.14) are rather generic results which go beyond our particular model. This assumption seems reasonable[15] as these general features basically depend on large N_c and on the hierarchy of exponentials (3.20) controlling the different contributions in eqs. (3.16)–(3.19). In turn, this depends only on the fact that large-N_c duality violations are concentrated on the real axis in the complex q^2 plane.

[14] See also ref. [11].
[15] See also ref. [7].

Therefore, let us start by assuming a duality violation of the form given in eq. (3.34), with parameters κ, γ, α and β to be determined. We remind the reader that in eqs. (3.23), (3.24) the b terms are suppressed by inverse powers of s_0. Therefore, in a first approximation, it may be reasonable to completely neglect the b terms in these two equations and, through eq. (3.22), extract these parameters κ, γ, α and β by means of a simultaneous fit to eqs. (3.23), (3.24). Then the rest of coefficients $a_{6,8,\ldots}$ and $b_{6,8,\ldots}$ can be obtained from eqs. (3.25)–(3.27) in a straightforward way.

Just to illustrate how this would work in our model, we have determined the parameters in eq. (3.34) by doing this simultaneous fit in the window $1.5\,\mathrm{GeV}^2 \leq s_0 \leq 3.5\,\mathrm{GeV}^2$ with 20 equally-spaced points, with the following result:

$$\kappa = 0.026\,, \qquad \gamma = 0.591\,\mathrm{GeV}^{-2}\,, \qquad \alpha = 3.323 \qquad \text{and} \qquad \beta = 3.112\,\mathrm{GeV}^{-2}\,. \tag{3.40}$$

Figure 9 shows in the upper row the result of the fit to eqs. (3.23), (3.24). As one can see, the overall fit is quite good. And since it improves in the intermediate region of the fitting window where both $\mathcal{D}^{[0]}$ and $\mathcal{D}^{[1]}$ have a zero, this suggests that a good strategy is to determine the OPE at these zeros. This is what we will do next.

In the lower row of figure 9, the dashed curve is the result for $\mathcal{D}^{[2,3]}(s_0)$ from the fitted function (3.34) and the solid curve is the result for the left-hand side of eqs. (3.25), (3.26), as calculated from the true values of the model.

Armed with eq. (3.34) and the values of the parameters from the fit (3.40), we predict a duality point s_0^* at which $\mathcal{D}^{[2]}(s_0^*) = 0$, within the window of our fit, to be at $s_0^* = 2.350\ \mathrm{GeV}^2$. Although similar, this value is not quite the same as the one obtained in the finite-energy sum rules analysis before, which was $2.363\,\mathrm{GeV}^2$. This small difference has a large impact on the determination of the OPE due to the steepness of the slope in the plot of figure 9 (lower curves), resulting in the large error quoted in the finite-energy sum rule analysis of eqs. (3.31), (3.32).

At this $s_0^* = 2.350\ \mathrm{GeV}^2$, on the other hand, one finds from eq. (3.25) that the OPE contribution is given by

$$\begin{aligned} a_6 + b_6 \log\frac{s_0^*}{\Lambda^2} + \frac{b_8}{s_0^*} - \frac{b_{10}}{2s_0^{*2}} &= \int_0^{s_0^*} dt\, t^2 \rho(t) \\ &= -0.00251\,\mathrm{GeV}^6\,, \end{aligned} \tag{3.41}$$

whereas the exact number for the combination on the left-hand side of eq. (3.41) obtained in the model is $-0.00281\,\mathrm{GeV}^2$, i.e. a $\sim 10\%$ error.[16] The same analysis can be repeated for the combinations appearing in the rest of eqs. (3.26), (3.27). For instance, we obtain

$$a_8 + b_8 \log\frac{s_0^*}{\Lambda^2} - b_6\, s_0^* + \frac{b_{10}}{s_0^*} = -\int_0^{s_0^*} dt\ t^3 \rho(t) = 0.00329\,\mathrm{GeV}^8 \qquad (s_0^* = 2.307\,\mathrm{GeV}^2)\,, \tag{3.42}$$

[16]We have repeated the analysis including the true values for the coefficients b_6 and b_8 in the fit to eqs. (3.23), (3.24). In this case the error becomes 14%.

JHEP08(2005)076

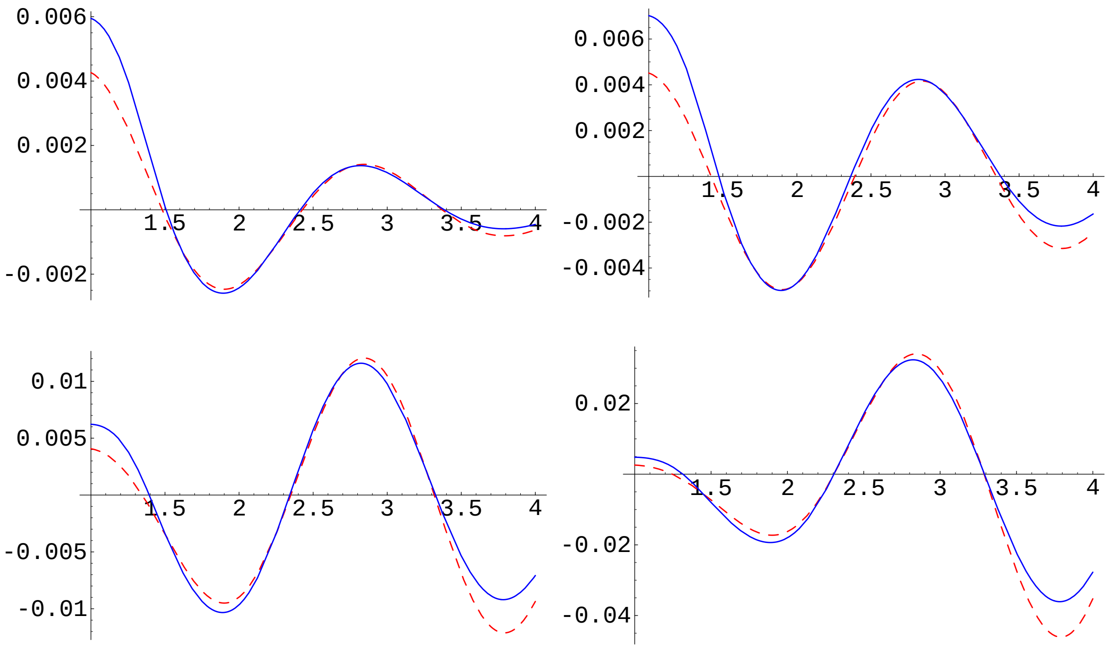

Figure 9: Upper row: Plot of the left-hand side (solid line) and fit of the right-hand side (dashed line) of eqs. (3.23), (3.24), neglecting the b coefficients, as a function of s_0 (in GeV^2). Lower row: Plot of the left-hand side (solid line) and right-hand side predicted by the fit (dashed line) of eqs. (3.25), (3.26), as a function of s_0 (in GeV^2).

and

$$a_{16} + b_{16} \log \frac{s_0^*}{\Lambda^2} - \frac{b_6 s_0^{*5}}{5} + \frac{b_8 s_0^{*4}}{4} - \frac{b_{10} s_0^{*3}}{3} + \frac{b_{12} s_0^{*2}}{2} - b_{14} s_0^* + \frac{b_{18}}{s_0^*} =$$
$$= - \int_0^{s_0^*} dt\ t^7 \rho(t) = 0.0179\,\mathrm{GeV}^{16} \qquad (s_0^* = 2.130\,\mathrm{GeV}^2)\,, \tag{3.43}$$

to be compared to the exact values on the left-hand sides of eqs. (3.42) and (3.43) which are $0.00344\,\mathrm{GeV}^8$ and $0.0161\,\mathrm{GeV}^{16}$, representing $\sim 4\%$ and $\sim 11\%$ errors, respectively. The gain in precision with respect to previous methods is clear.

4. Conclusion

We have developed a model of duality violations that shares many properties with QCD, including the fact that resonances in the real world have a non-vanishing width. Of course, an analysis of duality violations in a model cannot replace a similar analysis in QCD. For example, the precision of the determination of combinations of OPE coefficients in eqs. (3.41)–(3.43) is not necessarily an indication of what can be achieved in QCD. However, we do believe that the lessons from our model analysis are also relevant for QCD. First, the properties of the model that lead to duality violations are also present in QCD [7], notably the fact that the OPE in both is (at best) asymptotic. Second, because of the semi-realistic

JHEP08(2005)076

properties of the model, our analysis gives a good indication of the nature of systematic errors which result from making the various *ansätze* which have been proposed in the literature in order to deal with duality violations. We think that it should prove useful to attempt an analysis of the duality violations represented by the $\mathcal{D}^{[n]}$ (cf. eqs. (3.23)–(3.27)), using an *ansatz* similar to that of eq. (3.34), also in the QCD case. In addition, we would like to call the reader's attention to the additional contributions to the "OPE side" of duality relations, represented by the b_{2n} in eqs. (3.23)–(3.27). While some of the b_{2n} may be small in the case of QCD, there are contributions proportional to positive powers of s_0, which enhance the effects of the b_{2n} coefficients. To the best of our knowledge, this issue has not been taken into account in any of the previous determinations in the literature of higher-dimension OPE coefficients from duality. In a realistic analysis of the data, the procedure probably should be refined to determine all the a and b coefficients of the OPE, as well as the parameters κ, γ, α and β of eq. (3.34) parameterizing the duality violations, by means of a simultaneous fit to all eqs. (3.23)–(3.27), in a manner similar to that of ref. [20].

Finally, in real life one will also have to deal with experimental error bars, of course. For example, the experimental error bars in figure 5 are large in the large-s_0 region, and this will further complicate a precision determination of OPE coefficients. However, we hope to have made it clear that much can be learned from considering models such as the one analyzed in this paper, and that some of the lessons can be applied to the real-world case of QCD. At the very least, an analysis like the one presented here offers a way to estimate systematic effects.

Acknowledgments

We would like to thank Hans Bijnens, Vincenzo Cirigliano, Eduardo de Rafael, John Donoghue, Matthias Jamin, Jose Ignacio Latorre, Ximo Prades and Joan Rojo for discussions. MG thanks the IFAE at the Universitat Autònoma de Barcelona, and SP thanks the Dept. of Physics at San Francisco State University for hospitality. All three of us thank the Benasque Center for Science for hospitality. OC and SP are supported by CICYT-FEDER-FPA2002-00748, 2001-SGR00188 and by TMR, EC-Contract No. HPRN-CT-2002-00311 (EURIDICE). MG is partially supported by the US Dept. of Energy.

A. OPE asymptotic behavior

The OPE of our model stems from the asymptotic expansion of the $\psi(z)$ function in eq. (2.25). Using the identity for Bernoulli numbers

$$B_{2n} = 2\,(-1)^{n+1}\frac{(2n)!}{(2\pi)^{2n}}\,\zeta(2n)\,, \qquad n = 1, 2, 3, \ldots \tag{A.1}$$

where $\zeta(2n)$ is Riemann's zeta function, one can estimate the minimal error, δ, for this expansion as

$$\delta \sim \frac{B_{2n^*}}{2n^* z^{2n^*}} \tag{A.2}$$

where n^* is the optimal value in the sum (2.25). This n^*, in turn, can be estimated as the value at which two consecutive terms in the sum (2.25) are approximately equal. This results in $n^* \sim \pi z$.

Consequently, after using Stirling's expression for the factorial, one obtains for the minimum error in the asymptotic expansion (2.25)

$$\delta \sim e^{-2\pi z} , \tag{A.3}$$

where, here, $z \sim (|q^2|/\Lambda^2)^\zeta$ at large $|q^2|$, and $\zeta = 1 - a/\pi N_c$ for finite N_c. The estimate (A.3) is also valid for the function $\Pi_{VV} - \Pi_{AA}$, because there is no cancelation in the difference after inclusion of the right pre-factors. The result (A.3) is what appears in eqs. (2.27) and (3.6) in the main text.

We use the opportunity to also give some details of the derivation of eq. (3.19).

From its definition (2.32), $\mathcal{D}^{[n]}_{\text{const.}}(s_0)$ can be written as

$$\mathcal{D}^{[n]}_{\text{const.}}(s_0) = \mathcal{C}^{[n]} + \frac{1}{2\pi i} \left\{ \int_{-i\infty}^{-is_0} + \int_{is_0}^{i\infty} \right\} dq^2 \; q^{2n} \Delta(q^2) \, . \tag{A.4}$$

The two integrals can be estimated by using the large-q^2 behavior of $\Delta(q^2)$, if s_0 is large. Referring back to eq. (3.7), we note that

$$\cot \left[\pi \left(\frac{-q^2}{\Lambda^2} \right)^\zeta + \pi \frac{m^2}{\Lambda^2} \right] = 2e^{-2y} \; \sin(2x) \pm i \left(1 + 2e^{-2y} \; \cos(2x) \right) + \mathcal{O}\left(e^{-4y} \right) , \tag{A.5}$$

where the plus (minus) sign should be used on the positive (negative) imaginary axis, and where we defined

$$\begin{aligned} x &= \pi \left| \frac{q^2}{\Lambda^2} \right|^\zeta \cos \left(\frac{\zeta\pi}{2} \right) + \pi \frac{m^2}{\Lambda^2} , \\ y &= \pi \left| \frac{q^2}{\Lambda^2} \right|^\zeta \sin \left(\frac{\zeta\pi}{2} \right) . \end{aligned} \tag{A.6}$$

It is then straightforward to estimate each integral by using the bounds $|\sin(2x)| \leq 1$, $|\cos(2x)| \leq 1$, and taking $\zeta \to 1$. The unsuppressed $\pm i$ in eq. (A.5) cancels between the vector and axial channels, and we obtain the result given in eq. (3.19).

References

[1] M.A. Shifman, A.I. Vainshtein and V.I. Zakharov, *QCD and resonance physics. Sum rules*, *Nucl. Phys.* **B 147** (1979) 385.

[2] M. Knecht, S. Peris and E. de Rafael, *Matrix elements of electroweak penguin operators in the $1/N_c$ expansion*, *Phys. Lett.* **B 457** (1999) 227 [hep-ph/9812471];
J.F. Donoghue and E. Golowich, *Dispersive calculation of $B_7^{(3/2)}$ and $B_8^{(3/2)}$ in the chiral limit*, *Phys. Lett.* **B 478** (2000) 172 [hep-ph/9911309];
M. Knecht, S. Peris and E. de Rafael, *A critical reassessment of Q_7 and Q_8 matrix elements*, *Phys. Lett.* **B 508** (2001) 117 [hep-ph/0102017].

[3] R. Shankar, *Determination of the quark - gluon coupling constant*, *Phys. Rev.* **D 15** (1977) 755.

[4] For a review see, e.g. E. de Rafael, *An introduction to sum rules in QCD*, hep-ph/9802448.

[5] E. Braaten, S. Narison and A. Pich, *QCD analysis of the tau hadronic width*, *Nucl. Phys.* **B 373** (1992) 581.

[6] G. 't Hooft, *A planar diagram theory for strong interactions*, *Nucl. Phys.* **B 72** (1974) 461; E. Witten, *Baryons in the* $1/n$ *expansion*, *Nucl. Phys.* **B 160** (1979) 57.

[7] M.A. Shifman, *Quark-hadron duality*, hep-ph/0009131.

[8] See, e.g. V.I. Zakharov, *Non-perturbative match of ultraviolet renormalon*, hep-ph/0309178.

[9] M. Golterman and S. Peris, *Large-N_c QCD meets Regge theory: the example of spin-one two-point functions*, *JHEP* **01** (2001) 028 [hep-ph/0101098].

[10] M. Golterman and S. Peris, *On the use of the operator product expansion to constrain the hadron spectrum*, *Phys. Rev.* **D 67** (2003) 096001 [hep-ph/0207060].

[11] M. Golterman, S. Peris, B. Phily and E. De Rafael, *Testing an approximation to large-N_c QCD with a toy model*, *JHEP* **01** (2002) 024 [hep-ph/0112042].

[12] S.S. Afonin, A.A. Andrianov, V.A. Andrianov and D. Espriu, *Matching Regge theory to the ope*, *JHEP* **04** (2004) 039 [hep-ph/0403268].

[13] Discussion session led by J. Donoghue at the workshop *Matching light quarks to hadrons*, Benasque Center for Science, Benasque, Spain, July-August 2004, http://benasque.ecm.ub.es/2004quarks/2004quarks.htm.

[14] See, e.g. S. Bethke, *α_s at Zinnowitz 2004*, *Nucl. Phys.* **135** *(Proc. Suppl.)* (2004) 345 [hep-ex/0407021].

[15] See, e.g. R. Gupta, *Estimates of light quark masses from lattice QCD and QCD sum rules*, *ECONF* **C0304052** (2003) WG503 [hep-ph/0311033];
For a recent determination see E. Gamiz, M. Jamin, A. Pich, J. Prades and F. Schwab, *V_{us} and m_s from hadronic τ decays*, *Phys. Rev. Lett.* **94** (2005) 011803 [hep-ph/0408044];
discussion session led by C. Bernard at the workshop *Matching light quarks to hadrons*, Benasque Center for Science, Benasque, Spain, July-August 2004, http://benasque.ecm.ub.es/2004quarks/2004quarks.htm.

[16] ALEPH collaboration, R. Barate et al., *Measurement of the spectral functions of axial-vector hadronic τ decays and determination of $\alpha_s(M_\tau^2)$*, *Eur. Phys. J.* **C 4** (1998) 409;
OPAL collaboration, K. Ackerstaff et al., *Measurement of the strong coupling constant α_s and the vector and axial-vector spectral functions in hadronic tau decays*, *Eur. Phys. J.* **C 7** (1999) 571 [hep-ex/9808019];
S. Peris, B. Phily and E. de Rafael, *Tests of large-N_c QCD from hadronic τ decay*, *Phys. Rev. Lett.* **86** (2001) 14 [hep-ph/0007338];
S. Friot, D. Greynat and E. de Rafael, *Chiral condensates, Q_7 and Q_8 matrix elements and large-N_c QCD*, *JHEP* **10** (2004) 043 [hep-ph/0408281];
M. Davier, L. Girlanda, A. Hocker and J. Stern, *Finite energy chiral sum rules and τ spectral functions*, *Phys. Rev.* **D 58** (1998) 096014 [hep-ph/9802447];
B.L. Ioffe and K.N. Zyablyuk, *The V-A sum rules and the operator product expansion in complex Q^2-plane from τ decay data*, *Nucl. Phys.* **A 687** (2001) 437 [hep-ph/0010089];

JHEP08(2005)076

K.N. Zyablyuk, *VA sum rules with D=10 operators*, *Eur. Phys. J.* **C 38** (2004) 215 [hep-ph/0404230];
J. Bijnens, E. Gamiz and J. Prades, *Matching the electroweak penguins Q_7, Q_8 and spectral correlators*, *JHEP* **10** (2001) 009 [hep-ph/0108240];
C.A. Dominguez and K. Schilcher, *Finite energy chiral sum rules in QCD*, *Phys. Lett.* **B 581** (2004) 193 [hep-ph/0309285];
J. Rojo and J.I. Latorre, *Neural network parametrization of spectral functions from hadronic τ decays and determination of QCD vacuum condensates*, *JHEP* **01** (2004) 055 [hep-ph/0401047];
V. Cirigliano, E. Golowich and K. Maltman, *QCD condensates for the light quark V-A correlator*, *Phys. Rev.* **D 68** (2003) 054013 [hep-ph/0305118];
S. Ciulli, C. Sebu, K. Schilcher and H. Spiesberger, *QCD condensates from tau decay data: a functional approach*, *Phys. Lett.* **B 595** (2004) 359 [hep-ph/0312212].

[17] S. Narison, *V-A hadronic τ decays: a laboratory for the QCD vacuum*, hep-ph/0412152.

[18] P. Boucaud et al., *An exploratory lattice study of $\Delta I = 3/2 K \to \pi\pi$ decays at next-to-leading order in the chiral expansion*, *Nucl. Phys.* **B 721** (2005) 175 [hep-lat/0412029].

[19] G. 't Hooft, *A two-dimensional model for mesons*, *Nucl. Phys.* **B 75** (1974) 461;
C.G. Callan Jr., N. Coote and D.J. Gross, *Two-dimensional Yang-Mills theory: a model of quark confinement*, *Phys. Rev.* **D 13** (1976) 1649;
M.B. Einhorn, *Form-factors and deep inelastic scattering in two- dimensional quantum chromodynamics*, *Phys. Rev.* **D 14** (1976) 3451.

[20] V. Cirigliano, E. Golowich and K. Maltman, *QCD condensates for the light quark V-A correlator*, *Phys. Rev.* **D 68** (2003) 054013 [hep-ph/0305118].

[21] V. Cirigliano, J.F. Donoghue, E. Golowich and K. Maltman, *Determination of $\langle(\pi\pi)_{I=2}|Q_{7,8}|K^0\rangle$ in the chiral limit*, *Phys. Lett.* **B 522** (2001) 245 [hep-ph/0109113];
See also ref. [23].

[22] S. Peris, B. Phily and E. de Rafael, *Tests of large-N_c QCD from hadronic τ decay*, *Phys. Rev. Lett.* **86** (2001) 14 [hep-ph/0007338].

[23] J. Bijnens, E. Gamiz and J. Prades, *Matching the electroweak penguins Q_7, Q_8 and spectral correlators*, *JHEP* **10** (2001) 009 [hep-ph/0108240].

[24] J. Rojo and J.I. Latorre, *Neural network parametrization of spectral functions from hadronic tau decays and determination of QCD vacuum condensates*, *JHEP* **01** (2004) 055 [hep-ph/0401047].

[25] C.A. Dominguez and K. Schilcher, *Finite energy chiral sum rules in QCD*, *Phys. Lett.* **B 581** (2004) 193 [hep-ph/0309285].

[26] For a review see, e.g. S. Peris, *Electroweak matrix elements at large-N_c: matching quarks to mesons*, hep-ph/0204181;
E. de Rafael, *Analytic approaches to Kaon physics*, *Nucl. Phys.* **119** *(Proc. Suppl.)* (2003) 71 [hep-ph/0210317];
discussion sessions led by M. Knecht and E. de Rafael at the workshop *Matching light quarks to hadrons*, Benasque Center for Science, Benasque, Spain, July-August 2004, http://benasque.ecm.ub.es/2004quarks/2004quarks.htm;
S. Peris, *Kaon weak interactions in powers of $1/N_c$*, hep-ph/0411308.

[27] S. Friot, D. Greynat and E. de Rafael, *Chiral condensates, Q_7 and Q_8 matrix elements and large-N_c QCD*, *JHEP* **10** (2004) 043 [hep-ph/0408281].